

1 **HIV-1 Vpr antagonizes innate immune activation by targeting karyopherin-mediated NF-**
2 **κB/IRF3 nuclear transport**

3

4 Hataf Khan^{1,2,+}, Rebecca P. Sumner^{1,+}, Jane Rasaiyaah^{1,3}, Choon Ping Tan^{1,4}, Maria Teresa
5 Rodriguez-Plata^{1,5}, Chris van Tulleken¹, Douglas Fink¹, Lorena Zuliani-Alvarez¹, Lucy Thorne¹,
6 David Stirling^{1,6} Richard S. B. Milne¹ & Greg J. Towers¹

7

8 ¹Division of Infection and Immunity, University College London, 90 Gower Street, London, UK

9 ²Current address: Department of Infectious Diseases, King's College London, London, UK

10 ³Current address: Molecular and Cellular Immunology Unit, UCL Great Ormond Street Institute of
11 Child Health, London, UK.

12 ⁴Current address: Translation & Innovation Hub, 80 Wood Lane, London, UK

13 ⁵Current address: Black Belt TX Ltd, Stevenage Bioscience Catalyst, Gunnels Wood Rd,
14 Stevenage, UK

15 ⁶Current address: Broad Institute of MIT and Harvard University, Cambridge, MA, USA.

16 ⁺equal contribution

17 ^{*}Correspondence: g.towers@ucl.ac.uk

18

19 **Abstract**

20 HIV-1 must replicate in cells that are equipped to defend themselves from infection through
21 intracellular innate immune systems. HIV-1 evades innate immune sensing through encapsidated
22 DNA synthesis and encodes accessory genes that antagonize specific antiviral effectors. Here we
23 show that both particle associated, and expressed HIV-1 Vpr, antagonize the stimulatory effect of
24 a variety of pathogen associated molecular patterns by inhibiting IRF3 and NF-κB nuclear
25 transport. Phosphorylation of IRF3 at S396, but not S386, was also inhibited. We propose that,
26 rather than promoting HIV-1 nuclear import, Vpr interacts with karyopherins to disturb their import
27 of IRF3 and NF-κB to promote replication in macrophages. Concordantly, we demonstrate Vpr
28 dependent rescue of HIV-1 replication in human macrophages from inhibition by cGAMP, the
29 product of activated cGAS. We propose a model that unifies Vpr manipulation of nuclear import
30 and inhibition of innate immune activation to promote HIV-1 replication and transmission.

31

32 Key words: HIV-1, Vpr, DNA sensing, cGAS, Karyopherin, IRF3, NF- κB, nuclear transport

33

34

35

36

37

38

39 Introduction

40 Like all viruses, lentiviruses must navigate the hostile environment of the host cell in order to infect,
41 produce new viral particles, and transmit to new cells. A principal feature of cellular defences is
42 detection or sensing of incoming viruses and subsequent production of inflammatory cytokines,
43 particularly type 1 interferons (IFNs). All viral infections likely trigger IFN *in vivo* and the degree to
44 which they do this, and their capacity to antagonize IFN activity and its complex effects, are key in
45 determining transmission mechanism, host range and disease pathogenesis. Like other viruses,
46 lentiviruses antagonize specific host proteins or pathways that would otherwise suppress infection.
47 Lentiviruses typically do this through accessory gene function. For example, HIV-1 antagonizes
48 IFN induced restriction factors through accessory genes encoding Vif (APOBEC3G/H), Vpu
49 (tetherin) and Nef (tetherin/SERINC3/5) reviewed in (Foster et al., 2017; Sumner et al., 2017).

50
51 The role of the HIV-1 accessory protein Vpr has been less clearly defined. Manipulation of host
52 innate immune mechanisms by Vpr to facilitate replication in macrophages has been suggested
53 by several studies although there is still no clear model of mechanism and understanding of the
54 target proteins that link Vpr to innate immune manipulation is limited (Harman et al., 2015; Liu et
55 al., 2014; Okumura et al., 2008; Trotard et al., 2016; Vermeire et al., 2016). Vpr clearly changes
56 infected cell protein profiles affecting the level of hundreds of proteins in proteomic studies, likely
57 indirectly in most cases, suggesting manipulation of central mechanisms in cell biology
58 (Greenwood et al., 2019). There is also evidence for Vpr interacting with and manipulating many
59 specific proteins including its cofactor DCAF1 (Zhang et al., 2001), karyopherin alpha 1 (KPNA1,
60 importin α) (Miyatake et al., 2016) the host enzyme UNG2 (Wu et al., 2016) as well as HTLF
61 (Lahouassa et al., 2016; Yan et al., 2019), SLX4 (Laguetta et al., 2014) and CCDC137 (Zhang &
62 Bieniasz, 2019). Vpr has also been shown to both enhance (Liu et al., 2014; Liu et al., 2013;
63 Vermeire et al., 2016) decrease, NF- κ B activation (Harman et al., 2015; Trotard et al., 2016) in
64 different contexts and act as a cofactor for HIV-1 nuclear entry, particularly in macrophages
65 (Vodicka et al., 1998). However, despite this work the mechanistic details of Vpr promotion of HIV
66 replication are poorly understood and many studies seem contradictory. This is partly because the
67 mechanisms of Vpr-dependent enhancement of HIV-1 replication are context dependent, and cell
68 type specific although most studies agree that Vpr is more important for replication in macrophages
69 than in T cells or PBMC (Connor et al., 1995; Dedera et al., 1989; Fouchier et al., 1998; Hattori et
70 al., 1990; Mashiba et al., 2014)

71
72 In this paper, we demonstrate that Vpr mutants, unable to recruit to the nuclear envelope, fail to
73 antagonize innate sensing, but retain induction of cell cycle arrest, genetically separating key Vpr
74 functions. We provide evidence that Vpr prevents IRF3 and NF- κ B from interacting with
75 karyopherin alpha 1 (KPNA1/importin α), thus inhibiting innate immune activation by viral and non-
76 viral agonists. Our new findings support a unifying model of Vpr function, consistent with much of

77 the Vpr literature, in which Vpr associated with incoming viral particles suppresses nuclear entry
78 of activated inflammatory transcription factors to facilitate HIV-1 replication in innate immune
79 activated macrophages.

80

81

82 **Results**

83 **HIV-1 replication in cGAMP-stimulated MDMs requires Vpr**

84 A considerable body of evidence suggests an important role for Vpr in supporting HIV-1 replication
85 in macrophages but the relevant Vpr mechanisms for this function have been enigmatic. We set
86 out to investigate the role of Vpr in manipulating host innate immune mechanisms during HIV-1
87 infection of primary human cells. We prepared human monocyte-derived macrophages (MDM) by
88 purifying monocytes from peripheral blood by adherence and treating with M-CSF (Rasaiyaah et
89 al., 2013). Macrophages prepared in this way are particularly permissive to HIV-1 replication
90 facilitating study of HIV-1 biology in a primary myeloid cell type. We found that wild type HIV-1 and
91 HIV-1 Δ Vpr replicated equally well in (MDM)(Figure 1A) (Rasaiyaah et al., 2013) Consistent with
92 previous studies, Wild type HIV-1, and HIV-1 deleted for Vpr replicated equally well in activated
93 primary human CD4+ T cells (Figure S1A) (Dedera et al., 1989; Fouchier et al., 1998).

94

95 Vpr has been shown to antagonize innate immune signaling in HeLa cells reconstituted for DNA
96 sensing by STING expression (Trotard et al., 2016), so we hypothesized that Vpr might be
97 particularly important when DNA sensing is activated. To test this, we mimicked activation of the
98 DNA sensor cGAS by treating MDM with cGAMP, the product of activated cGAS. In the presence
99 of cGAMP, HIV-1 replication in MDM was, indeed, Vpr-dependent. 1 μ g/ml cGAMP specifically
100 suppressed HIV-1 Δ Vpr more potently than wild type virus and 4 μ g/ml cGAMP overcame Vpr
101 activity and suppressed replication of both wild type and mutant viruses (Figure 1A). Intriguingly,
102 Vpr did not rescue HIV-1 replication from cGAMP-mediated inhibition in primary human CD4+ T
103 cells, and cGAMP had only minimal effect on HIV-1 replication in Jurkat T cells (Figure S1A).
104 These data demonstrate that HIV-1 replication in cGAMP-stimulated MDM is Vpr dependent. They
105 are consistent with previous observations suggesting Vpr is more important in macrophages than
106 T cells and that the consequences of cGAMP treatment differ between these cell types (Gulen et
107 al., 2017; Xu et al., 2016).

108

109 **HIV-1 particle delivered Vpr inhibits gene expression stimulated by DNA sensing**

110 We next investigated the effect of particle-associated Vpr on innate immune activation. The
111 myeloid cell line THP-1 expresses cGAS and STING and has a functional DNA sensing pathway
112 (Mankan et al., 2014). We used THP-1 cells expressing the Gaussia luciferase gene under the
113 control of the endogenous *IFIT1* promoter (herein referred to as THP-1 IFIT1-luc) (Mankan et al.,
114 2014) to measure the effect of Vpr on cGAMP-induced IFIT1-luc expression. IFIT1 (ISG56) is a

115 well-characterized ISG that is highly sensitive to cGAMP and type 1 IFN. Treatment of THP-1
116 IFIT-luc cells with cGAMP induced IFIT1-luc expression by two orders of magnitude. This activation
117 was significantly suppressed if cells were infected with VSV-G pseudotyped, genome-free, HIV-
118 particles bearing Vpr, (referred to here as virus-like particles or VLP), but not by VLP lacking Vpr,
119 immediately prior to cGAMP addition (Figure 1B). IFIT1-Luc was measured 6, 8 and 24 hours after
120 cGAMP addition/infection.

121

122 In this experiment, doses of VLP required to suppress IFIT1-luc expression were high, equivalent
123 to a multiplicity of infection of 20 as measured by correlating VLP reverse transcriptase levels (SG-
124 PERT) (Jolien Vermeire et al., 2012), with HIV-1 GFP titers on THP-1. We assume that such a
125 high dose of Vpr-bearing VLP is required because cGAMP treatment activates numerous STING
126 complexes in most of the cGAMP-treated cells. If this effect of Vpr is relevant to infection, we
127 expect that cGAS/STING activated by the incoming HIV genome should be sensitive to the amount
128 of Vpr contained in an individual particle. To test this, we activated DNA sensing using high dose
129 infection by VSV-G pseudotyped HIV-1 vectors bearing GFP-encoding genome. We used an HIV-
130 1 packaging plasmid, derived from HIV-1 clone R9, encoding Gag-Pol, Tat and Rev (p8.91) or
131 Gag-Pol, Tat and Rev and Vpr, Vpu, Vif and Nef (p8.2) (Zufferey et al., 1997). Strikingly, although
132 Vpr positive and negative HIV-1 GFP stocks infected THP-1 cells to similar levels (Figure 1D),
133 induction of inflammatory cytokine, and ISG, CXCL10 was reduced if the HIV-1 GFP carried Vpr
134 (Figure 1C). This indicates that Vpr can inhibit the consequences of sensing driven by the Vpr
135 bearing virus particles themselves.

136

137 Genome-free, non-infectious, HIV-1 particles did not induce CXCL10 expression (Figure 1E, F),
138 evidencing the importance of viral DNA in this response. Furthermore, CXCL10 expression was
139 not induced after infection of THP-1 cGAS knock out cells, consistent with CXCL10 induction being
140 cGAS-dependent. Knock out of the RNA sensing adaptor protein MAVS had no effect on induction
141 of CXCL10 (Figure 1G). cGAS and MAVS knock out were confirmed by immunoblot (Figure S1C).

142

143 As expected, a lower dose of virus was required to see the effect of Vpr when the particles
144 themselves activated sensing, and in this latter experiment, Vpr effects were clear at MOIs of 3
145 (Figure 1C, E). Moreover, single round titer of HIV-1 GFP was not affected by cGAS or MAVS
146 knock out, confirming that sensing activation does not impact single round infectivity of HIV-1 GFP
147 VSV-G pseudotypes in this assay consistent with HIV-1 vector not being particularly sensitive to
148 IFN (Figure 1H, Figure S1B).

149

150 **HIV-1 Vpr expression inhibits innate immune activation**

151 We next tested whether Vpr expressed in isolation can suppress innate immune activation by
152 cGAMP. Vpr from the primary founder HIV-1 clone SUMA (Fischer et al., 2010) was expressed in

153 THP-1 IFIT1-luc cells using an HIV-1 vector we called pCSVIG (Figure S2A, S2B). Vpr was
154 expressed using MOIs of approximately 0.2-1. Forty hours after transduction, cells were treated
155 with cGAMP (5µg/ml), and IFIT1-luc was measured 8 hours later. Prior expression of Vpr reduced
156 IFIT1-luc responses in a dose-dependent manner whilst the highest dose of empty vector had no
157 effect (Figure 2A). Vpr expression (MOI=1, Figure S2C) also suppressed cGAMP-mediated
158 induction of endogenous ISG mRNA expression, measured by qRT-PCR for *MxA*, *CXCL10*, *IFIT2*
159 and *viperin* (Figure 2B) and inhibited cGAMP induced CXCL10 secretion (Figure 2C; infection data
160 in Figure S2D).

161

162 IFIT1-luc expression stimulated by transfection of herring testis (HT) DNA was also inhibited by
163 Vpr expression, consistent with the notion that Vpr antagonizes DNA sensing (Figure 2D, Figure
164 S2E). Strikingly, Vpr also reduced Sendai virus induced activation of IFIT1-luc, which is mediated
165 by MDA5 and RIGI RNA sensing (Andrejeva et al., 2004; Rehwinkel et al., 2010) (Figure 2E, Figure
166 S2G) and IFIT1-luc activation after stimulation with the TLR4 ligand LPS (Figure 2F, S2H). Thus,
167 Vpr expression appeared to mediate a generalized suppression of innate immune activation.

168

169 **Vpr inhibition of innate immune activation is dependent on DCAF1 but independent of cell** 170 **cycle arrest**

171 In order to separate innate immune antagonism from other Vpr functions, we used three Vpr
172 mutants with distinct functional deficits. Vpr R80A, is defective in inducing cell cycle arrest
173 (Laguette et al., 2014); Vpr Q65R fails to recruit DCAF1 and so cannot degrade target proteins
174 (Laguette et al., 2014); and Vpr F34I/P35N fails to bind cyclophilin A and does not localize to the
175 nuclear membrane (Vodicka et al., 1998; Zander et al., 2003).

176

177 All three mutant Vprs were efficiently incorporated into HIV-1 GFP particles (Figure 3A). When
178 delivered by viral particles, Vpr R80A effectively suppressed IFIT1-luc induction by cGAMP in THP-
179 1 cells, however Vpr Q65R and Vpr F34I/P35N had little if any suppressive effect (Figure 3B). In
180 these experiments, cGAMP was added to the target cells directly after the virus. Suppression of
181 IFIT1-luc induction by Vpr R80A suggested that cell cycle arrest was not required for innate
182 immune antagonism. To further test this, we measured the effect of all three Vpr mutants on cell
183 cycle progression. As reported, WT Vpr expression in THP-1 cells induced a significant increase
184 of cells in G2/M phase of cell cycle and Vpr R80A had no effect (Figure 3C) (Laguette et al., 2014).
185 Vpr F34I/P35N, which cannot effectively suppress cGAMP mediated IFIT1-luc/ISG expression
186 (Figure 3B, 3G), also induced G1/M cell cycle arrest, albeit slightly less efficiently than wild type
187 Vpr protein, as previously described (Vodicka et al., 1998) (Figure 3C). The DCAF1 Vpr binding
188 mutant Q65R did not inhibit cell cycle, as reported (Figure 3C) (Laguette et al., 2014). These data
189 genetically separate the effects of Vpr expression on cell cycle, and on inhibition of innate immune
190 activation, suggesting that these functions depend on manipulation of different target proteins. It

191 is striking that amino acids at positions 34/35 and 80 are close in Vpr structures and distant from
192 the UNG2 binding site, suggesting an additional target binding interface, as seen in the highly
193 related Vpx protein (Figure S3B, C) (Morellet et al., 2003; Schwefel et al., 2014; Wu et al., 2016).

194

195 We next asked whether DCAF-1 was required for innate immune antagonism, as suggested by
196 the Vpr Q65R mutant, which fails to recruit DCAF1, and cannot suppress cGAMP-induced IFIT1-
197 luc expression (Figure 3B). Depletion of DCAF1 in THP-1 cells by shRNA prevented Vpr from
198 inhibiting cGAMP induction of IFIT1-luc (Figure 3D). Neither DCAF1 depletion, nor cGAMP
199 treatment reduced infectivity of HIV-1 GFP vector (Figure S3A). Vpr was active in cells expressing
200 a non-targeting shRNA (shControl) and suppressed IFIT1-luc induction. Expression of empty (no
201 Vpr) vector had no effect on IFIT1-luc induction (Figure 3D). Effective depletion of DCAF1 was
202 evidenced by immunoblot (Figure 3E). Thus, Vpr inhibition of innate immune activation requires
203 DCAF1.

204

205 Expressed Vpr had similar mutation sensitivity as Vpr delivered by HIV-1 particles (compare
206 Figures 3F, G and 3B). Expression of wild type Vpr, or Vpr R80A, prevented cGAMP activation of
207 the IFIT1-luc reporter (Figure 3F), and of endogenous *MxA* in THP-1 cells (Figure 3G, S3D). HT
208 DNA transfection, but not lipofectamine alone, activated IFIT1-luc reporter expression, as
209 expected, and this was also sensitive to wild type and VprR80A expression, but not expression of
210 Vpr F34I/P35N (Figure S3E, S3F). Vpr Q65R had only a small inhibitory effect consistent with data
211 in Figure 3B.

212

213 **Wild Type Vpr, but not sensing antagonism inactive Vpr mutants, colocalize with nuclear** 214 **pores**

215 Having identified Vpr mutants defective for antagonism of innate immune sensing, we sought
216 further clues about Vpr mechanism by examining wild type and mutant Vpr location within cells.
217 Vpr expressed in isolation is found in the nucleus and associated with nuclear pores (Fouchier et
218 al., 1998; Le Rouzic et al., 2002). Concordantly, we found FLAG-Vpr in the nucleus, and
219 colocalized with antibody staining the nuclear pore complex, when expressed by transient
220 transfection in HeLa cells (Figure 4A, B). As previously reported for the single mutant F34I (Jacquot
221 et al., 2007; Vodicka et al., 1998), we found that the double Vpr mutant F34I/P35N, as well as Vpr
222 Q65R, were mislocalized, as compared to wild type and R80A Vpr. Thus mutants which fail to
223 inactivate innate immune sensing, fail to localize to the nuclear membrane. Defective Vpr mutants
224 F34I/P35N and Q65R appeared qualitatively different inside the nucleus, and nuclear rim staining
225 was less well defined, suggesting that they have lost interactions with a protein(s) that normally
226 influences their position within the cell. Fluorescence intensity measurements along transverse
227 sections of nuclei in single confocal images showed two distinct peaks of nuclear pore staining
228 representing each edge of the nucleus. These peaks overlapped with WT and Vpr R80A

229 fluorescence but not with Vpr F34I/P35N or Vpr Q65R fluorescence, which was more diffuse and
230 less well defined at the nuclear rim (Figure 4C). These data link Vpr nuclear membrane association
231 with antagonism of innate immune sensing for the first time.

232

233 Vpr has been described to interact with cyclophilin A (CypA) and mutating Vpr residue P35 was
234 reported to prevent this interaction (Zander et al., 2003). The nuclear pore complex has cyclophilin-
235 like domains, which are structurally very similar to CypA, at the end of the Nup358 fibers that
236 protrude into the cytoplasm (Schaller et al., 2011). To test whether Nup358 was required for Vpr
237 association with the nuclear rim, we expressed FLAG-Vpr in Nup358-depleted HeLa cells (Schaller
238 et al., 2011) and stained the Vpr FLAG tag (green) and NPC (red) (Figure S4A, B). Despite effective
239 Nup358 depletion (Figure S4C), Vpr remained associated with the nuclear rim suggesting that
240 Nup358 is not required for Vpr nuclear rim association (Figure S4A, B, D).

241

242 **Vpr inhibits IRF3 nuclear translocation**

243 cGAMP is produced by activated cGAS and is recruited by STING, which then forms an active
244 kinase complex in which TBK1 phosphorylates STING, TBK1 itself, and the transcription factor
245 IRF3 (Liu et al., 2015; Zhang et al., 2019). IRF3 phosphorylation promotes nuclear translocation
246 and subsequent activation of gene expression including type 1 IFNs (Chen et al., 2008). As
247 expected, transfection of THP-1 IFIT1-luc cells with HT DNA induced phosphorylation of STING,
248 TBK1 and IRF3-S386 (Figure 5A). Measurement of IFIT1-luc expression, in the same samples,
249 three hours after stimulation, indicated induction of IFIT1-luc by HT DNA but not after prior Vpr
250 expression using a lentiviral vector (Figure 5B). Strikingly, Vpr expression for 48 hours did not
251 impact STING, TBK1 or IRF3 protein levels, or their phosphorylation status 3 hours after DNA
252 transfection, measuring IRF3 phosphorylation at S386 (Figure 5A). Empty vector expression had
253 no detectable effect on protein levels or phosphorylation (Figure 5A). Actin was detected as a
254 loading control and Vpr/empty vector were used at a vector MOI of about 1 (Figure S5A). A second
255 example of this experiment is presented in Figure S5B-E. IRF3 is phosphorylated at multiple sites
256 during activation including at IRF3 S-396. We therefore examined IRF3 S-396 phosphorylation
257 using a phospho-IRF3-S396 specific antibody and flow cytometry because this antibody didn't
258 work well by immunoblot. We found that in this case, Vpr delivery by VLP did reduce
259 phosphorylation of IRF3-S-396 after stimulation by either cGAMP or HT DNA in THP-1 cells (Figure
260 5C).

261

262 Given that Vpr is associated with the nuclear rim, and Vpr mutations that break antagonism of
263 innate sensing mislocalize Vpr, we hypothesized that rather than impacting levels of signaling
264 proteins, Vpr may act at nuclear pores to influence nuclear transport of inflammatory transcription
265 factors. This would be consistent with the broad innate immune antagonism that we have observed
266 (Figure 2), and with previous reports of Vpr influencing nuclear transport, for example, of viral

267 nucleic acids (Heinzinger et al., 1994; Miyatake et al., 2016; Popov et al., 1998), and inhibiting
268 sensing of HIV-1 (Trotard et al., 2016). We therefore investigated the effect of Vpr on cGAMP-
269 induced IRF3 nuclear translocation. THP-1 were differentiated with 50ng/ml phorbol-12 myristate
270 acetate (PMA) to attach them to glass for microscopy. In these experiments, VLP with or without
271 Vpr are used to infect cells immediately after they are treated with innate immune stimulants. IRF3
272 translocation is measured three hours later by immunofluorescent labeling. VSV-G pseudotyped
273 HIV-1 GFP bearing Vpr reduced cGAMP-stimulated IRF3 nuclear translocation in a dose-
274 dependent way whilst HIV-1 lacking Vpr had no effect (Figure 5D, E, S5F). These data are
275 consistent with a previous report in which Vpr suppressed nuclear transport of IRF3-GFP on HIV-
276 1 infection of HeLa cells in which DNA sensing had been reconstituted by expression of STING
277 (Trotard et al., 2016). Importantly, in our experiments in THP-1, suppression of IRF3 nuclear
278 translocation by Vpr was sensitive to Vpr mutation, with the same specificity as before (Compare
279 Figure 3, 4, 5F, S5G-J). HIV-1 GFP bearing Vpr F34I/P35N, or Vpr Q65R, failed to efficiently
280 suppress IRF3 nuclear localization after cGAMP stimulation (Figure 5F, S5G) or after transfection
281 of differentiated THP-1 with HT DNA (Figure 5G, S5H). Conversely, HIV-1 GFP bearing wild type
282 Vpr, or Vpr R80A, effectively suppressed IRF3 nuclear localization after stimulation with cGAMP
283 or HT DNA (Figure 5F, G S5G, H). Similar inhibition specificity by Vpr was also seen after activation
284 of IRF3 nuclear translocation by transfection with the RNA mimic poly I:C (Figure S5I, J). Thus,
285 suppression of IRF3 nuclear translocation correlates with the capacity of Vpr mutants to
286 antagonize innate immune activation.

287

288 **Vpr inhibits NF- κ B p65 nuclear translocation and NF- κ B sensitive plasmid expression**

289 DNA sensing by cGAS is known to activate NF- κ B as well as IRF3 (Fang et al., 2017). To test
290 whether Vpr influenced NF- κ B activation we repeated the experiment in Figure 1C-F but using
291 THP-1 cells bearing an NF- κ B -luciferase reporter (THP-1 NF- κ B-luc) (Figure 6A-C). VSV-G
292 pseudotyped HIV-1 GFP vector bearing Vpr minimally activated NF- κ B-luc expression, whereas
293 Vpr negative HIV-1 GFP activated NF- κ B-luc expression effectively (Figure 6A). Activation was
294 dependent on viral genome because similar doses of HIV-1 VLP, made without genome, did not
295 induce NF- κ B-luc expression (Figure 6A). Viral doses were equalized by measurement of RT
296 activity (SGPERT) (Jolien Vermeire et al., 2012). Vpr bearing, and Vpr negative, HIV-1 GFP were
297 equally infectious and genome-free VLP were not infectious, as expected (Figure 6B). VSV-G
298 pseudotyped HIV-1 GFP bearing Vpr, but not virus lacking Vpr, suppressed cGAMP-mediated
299 activation of the NF- κ B-sensitive gene *IL6* (Figure 6C). We could not detect NF- κ B nuclear
300 localization in THP-1 after cGAMP treatment, perhaps due to timing, so we tested mutant Vpr
301 specificity using poly I:C to stimulate NF- κ B nuclear localization. Again, we transfected
302 differentiated THP-1 cells, this time with Poly I:C and then immediately infected them with HIV-1
303 GFP bearing or lacking Vpr and fixed and stained for NF- κ B localisation three hours later. We
304 found Vpr inhibited NF- κ B nuclear localisation with similar sensitivity to mutation as for IRF3: VLP

305 bearing wild type Vpr or Vpr R80A inhibited NF- κ B nuclear localisation but VLP bearing Vpr
306 F34I/P35N or Vpr Q65R did not (Figure 6D, S6B).

307

308 Previous work has shown that Vpr inhibits the activity of the human CMV major immediate early
309 promoter (MIEP) (Liu et al., 2015). We hypothesized that this effect may be due to the dependence
310 of this promoter on NF- κ B (DeMeritt et al., 2004). As expected Flag-Vpr expression suppressed
311 GFP expression from a co-transfected CMV MIEP – GFP construct (Figure 6E) as well as several
312 other NF- κ B sensitive constructs expressing luciferase (Figure S6A). Importantly, Vpr mutants
313 F34I/P35N, and Vpr Q65R suppressed GFP expression much less effectively than WT Vpr, or Vpr
314 R80A, consistent with this effect being due to inhibition of NF- κ B nuclear entry (Figure 6E, S6D,
315 E). To probe this further, we used two constructs lacking NF- κ B binding sites in which GFP is
316 driven from the Ubiquitin C (Ub) promoter (Matsuda & Cepko, 2004) or from the elongation factor
317 1 alpha (EF1 α) promoter (Matsuda & Cepko, 2004). Expression of GFP from these constructs was
318 minimally affected by Vpr co-transfection, but GFP expression from the CMV MIEP was reduced
319 as before (Figure 6F). Importantly, CMV MIEP-GFP expression was induced by activation of NF-
320 κ B with exogenous tumour necrosis factor alpha (TNF α) whereas Ub-GFP and EF1 α -GFP were
321 not, providing further evidence that Vpr inhibition correlated with promoter sensitivity to NF- κ B
322 (Figure 6G, S6E-F). Thus, inhibition of NF- κ B nuclear transport by Vpr likely explains the
323 observation that Vpr suppresses expression from the CMV MIEP, but not promoters that are
324 independent of NF- κ B activity for expression. This is important because previous studies have
325 used Vpr co-transfection with CMV MIEP driven promoters to address Vpr function (Su et al.,
326 2019).

327

328 **HIV-1 Vpr interacts with karyopherins and inhibits NF- κ B (p65) and IRF3 recruitment**

329 WT Vpr suppresses nuclear entry of IRF3 and NF- κ B, but Vpr DCAF1 binding mutant Q65R does
330 not (Figure 5, 6). This suggested that Vpr might degrade particular nuclear transport proteins to
331 exert its effect. We therefore tested whether Vpr expression caused degradation of karyopherins
332 KPNA1, KPNA2, KPNA3, KPNA4, KPNA5, KPNA6 or KPNA1. We infected cells with Vpr encoding
333 HIV-1 vector, extracted total protein 48 hours after infection, and detected each protein using
334 immunoblot (Figure 7A). However, we did not detect reduced levels of any of these karyopherins.
335 It is possible that Vpr recruits karyopherins but does not degrade them. To test this, we sought
336 interaction between Vpr and karyopherins KPNA1, KPNA2 and KPNA3 by co-immunoprecipitation.
337 We found that immunoprecipitation of wild type HA-Vpr co-precipitated Flag-KPNA1, as has been
338 reported previously (Miyatake et al., 2016; Nitahara-Kasahara et al., 2007; Vodicka et al., 1998)
339 and to a lesser degree Flag-KPNA2 and Flag-KPNA3, but not Flag-tagged GFP (Figure 7B). In a
340 second experiment we tested whether KPNA1-3 interacted with the inactive Vpr mutant
341 F34I/P35N. WT Vpr interacted with KPNA1 as before, with less efficient interaction with KPNA2
342 and KPNA3 (Figure 7C). Importantly, KPNA1 interacted with the Vpr F34I/P35N only very weakly,

343 and much less than WT Vpr, consistent with the mutant's reduced activity in antagonizing innate
344 immune sensing (Figure 7C). Given that Vpr expression did not cause KPNA1 degradation, we
345 sought evidence for Vpr disturbing interactions between KPNA1 and IRF3 or NF- κ B p65. HA-IRF3
346 immunoprecipitated with Flag-KPNA1 as expected and this interaction was reduced by expression
347 of WT Vpr, but not inactive mutant Vpr F34I/P35N (Figure 7D). A competing immunoprecipitation
348 experiment with KPNA1 and NF- κ B p65 gave similar results. Immunoprecipitation of Flag-KPNA1
349 co-precipitated NF- κ B p65 and this was reduced by co-expression of WT Vpr, but not Vpr
350 F34I/P35N (Figure 7E). Thus, for the first time, we explain the interaction of Vpr with karyopherins,
351 by demonstrating that it prevents them from efficiently recruiting and transporting transcription
352 factors IRF3 and NF- κ B into the nucleus after innate immune activation. This finding provides a
353 mechanistic basis for the broad innate immune antagonism activity of Vpr and links manipulation
354 of nuclear transport with antagonism of innate immunity rather than with infection itself.

355

356 **Discussion**

357 Despite many studies investigating Vpr function, a clear mechanism for how HIV-1 Vpr promotes
358 replication in macrophages has not been forthcoming, partly because Vpr replication phenotypes
359 have not been clearly mechanistically linked to manipulation of specific target proteins. Early work
360 connected nuclear membrane association of Vpr with replication in macrophages but not T cells
361 (Connor et al., 1995; Dedera et al., 1989; Fouchier et al., 1998; Hattori et al., 1990; Mashiba et al.,
362 2014; Vodicka et al., 1998). Early work also separated the effect of Vpr on cell cycle from its
363 association with the nuclear envelope using Vpr mutants, particularly Vpr F34I, which, as confirmed
364 herein, suppressed cell cycle, but did not recruit to the nuclear membrane (Jacquot et al., 2007;
365 Vodicka et al., 1998). Vpr mutants that did not localise to the nuclear membrane did not promote
366 macrophage replication, leading the authors to reasonably conclude that Vpr contributed to nuclear
367 transport of the virus itself. This observation was consistent with the notion that a Vpr role
368 supporting nuclear entry is expected to be more important in non-dividing cells (macrophages),
369 than rapidly dividing cells (activated T cells). Vpr is also not typically required for infection of cell
370 lines, even if they are not dividing (Yamashita & Emerman, 2005). Vpr has been linked to nuclear
371 transport through karyopherin binding, but again, this function has not been clearly linked to a
372 mechanism of replication enhancement, other than the hypothetical connection between Vpr and
373 nuclear transport of the virus itself (Jacquot et al., 2007; Nitahara-Kasahara et al., 2007a; Popov
374 et al., 1998; Vodicka et al., 1998).

375

376 In complementary studies, Vpr has been associated with antagonism of innate immune sensing in
377 macrophages (Harman et al., 2015), T cells (Vermeire et al., 2016), as well as in HeLa cells
378 reconstituted for DNA sensing by STING expression (Trotard et al., 2016). Here we propose a
379 model that unifies Vpr's role in manipulating nuclear entry with its antagonism of innate immune
380 signalling. We propose that Vpr interacts with karyopherin KPNA1 (Figure 7) to inhibit nuclear

381 transport of activated IRF3 and NF- κ B (Figure 5-7) and subsequent gene expression changes
382 downstream of innate immune sensing (Figures 1-3). Thus, HIV-1 Vpr antagonizes the
383 consequences of innate immune activation by HIV-derived, and non-HIV derived PAMPs alike,
384 explaining its importance for maximal replication in macrophages because activated T cells, and
385 most cell lines, respond to innate immune agonists poorly, particularly DNA based PAMPs (Figure
386 1) (Cingöz & Goff, 2019; de Queiroz et al., 2019; Heiber & Barber, 2012; Xia et al., 2016; Xia et
387 al., 2016). We propose that previous demonstrations of Vpr dependent HIV-1 replication in
388 macrophages, that depended on Vpr-NPC association, or nuclear transport factors, are explained
389 by Vpr inhibition of innate immune sensing and subsequent antiviral responses (Jacquot et al.,
390 2007; Vodicka et al., 1998). For example, induction of an innate response by HIV-1 lacking Vpr
391 might be expected to suppress viral nuclear entry because MxB induction in macrophages by IFN
392 causes inhibition of HIV-1 nuclear entry (Goujon et al., 2013; Kane et al., 2013). Indeed, we
393 hypothesise that Vpr provides an *in vivo* replication advantage because activation of IRF3 and NF-
394 κ B induces expression of inflammatory cytokines, including type 1 IFNs, and subsequently
395 restriction factors for which HIV-1 does not encode antagonists. For example, in addition to MxB,
396 IFN induces IFITM1-3 (Foster et al., 2016) and TRIM5 α (Jimenez-Guardeño et al., 2019) all of
397 which can inhibit HIV-1. Concordantly, accidental infection of a lab worker with a Vpr-defective
398 HIV-1 isolate resulted in delayed seroconversion, suppressed viremia and normal T-cell counts
399 without need for anti-viral treatment (Ali et al., 2018).

400
401 In most of the experiments herein, and in previous studies of Vpr function in cell lines (Yamashita
402 & Emerman, 2005), Vpr did not impact infection of single round VSV-G pseudotyped HIV-1 vectors
403 encoding GFP. We propose that this is because if antiviral inflammatory responses, e.g. IFN, are
404 triggered at around the time of infection, either by exogenous signals, or by HIV-1 itself, then the
405 activated antiviral effectors are too slow to inhibit that infection, ie the expression of GFP from an
406 integrated provirus. Thus, a requirement for Vpr is only revealed by spreading infection assays in
407 innate competent cells such as macrophages, which can suppress replication of subsequent
408 rounds of infection.

409
410 We find that Vpr can promote HIV-1 replication, even if the innate immune stimulation does not
411 originate from an HIV-1 derived PAMP, here exemplified by cGAMP treatment (Figure 1). We found
412 that Vpr also antagonised the effects of exposure to LPS, RNA and DNA ligands, as well as other
413 viral infections, exemplified here by Sendai virus infection, which whilst not a human virus, potently
414 activates RNA sensing and IFN production in human macrophages (Matikainen et al., 2000)(Figure
415 2). We hypothesise that Vpr has evolved a mechanism of broad specificity innate immune inhibition
416 to allow suppression of signals connected indirectly to infection. For example, HIV seroconversion
417 has been associated with a cytokine storm (Stacey et al., 2009) and this may be mitigated by
418 particle associated Vpr. Association between escape from innate sensing and successful

419 transmission is suggested by evidence for generally low HIV transmission frequency (Shaw &
420 Hunter, 2012), HIV founder clones being particularly resistant to IFN (Iyer et al., 2017) as well as
421 the transmission associated cytokine cascade (Stacey et al., 2009). Concordantly, Vpu, Nef and
422 Vif, and Vpr, antagonize innate immunity to enhance viral replication, reviewed in Sumner et al.,
423 2019.

424

425 Vpr has been suggested to cause IRF3 degradation (Okumura et al., 2008) but we did not detect
426 IRF3 degradation in THP-1 cells under conditions when gene expression and IRF3 nuclear
427 transport were strongly suppressed (Figure 5). Furthermore, in addition to suppressing IRF3
428 nuclear transport, we found that Vpr reduced IRF3 phosphorylation at S396 but not at S386 (Figure
429 5). Previous studies have suggested that phosphorylation of IRF3 at S386 is necessary and
430 sufficient for IRF3 activation (Lin et al., 1999; Mori et al., 2004; Schirmmacher, 2015; Servant et al.,
431 2003; Suhara et al., 2000; Yoneyama et al., 1998). Thus our data are consistent with a more
432 complex picture of IRF3 activation by phosphorylation. It is possible that phosphorylation at S396
433 occurs in a karyopherin or NPC-dependent way that is occluded by Vpr recruitment to karyopherin.
434 Phosphorylation of IRF3 at S396 has been associated with enhanced association and
435 multimerization with transcriptional coactivator CREB binding protein (CBP/p300) suggesting a
436 later role than phosphorylation at S386 (Chen et al., 2008). It is possible that the lack of S396 IRF3
437 phosphorylation is a consequence of IRF3 dephosphorylation at S396 as nuclear entry is
438 prevented.

439

440 Inhibition of IRF3 phosphorylation is also consistent with reported inhibition of TBK1 by Vpr
441 although this study detected inhibition of TBK phosphorylation, whereas we did not (Harman et al.,
442 2015). In that study, Vpr promoted infection in macrophages and dendritic cells, despite HIV
443 induced formation of innate immune signalling complexes containing TBK1, IRF3 and TRAF3,
444 visualised by immunofluorescence staining. Thus TBK1 inhibition by Vpr may occur in addition to
445 Vpr activity on nuclear transport, because TBK1 is seen in the cytoplasm, not at the nuclear
446 envelope, in these HIV infected cells (Harman et al., 2015). IRF3 degradation was not detected in
447 this study and nor was HIV-1 induced IRF3 phosphorylation, although the impact of infection on
448 IRF3 by wild type HIV-1 and HIV-1 deleted for Vpr were not compared.

449

450 The regulation of the nuclear import of NF- κ B and IRF3 by multiple karyopherins is expected to be
451 complex (Fagerlund et al., 2005, 2008; Kumar et al., 2002; Liang et al., 2013). Targeting
452 karyopherins is a typical viral strategy for manipulation of cellular responses but the different ways
453 viruses perform this function hints at the complexity required to inhibit innate responses whilst
454 avoiding shutting down viral transcription. For example, Japanese encephalitis virus NS5 targets
455 KPNA2, 3 and 4 to prevent IRF3 and NF- κ B nuclear translocation (Ye et al., 2017). Hantaan virus
456 nucleocapsid protein inhibits NF- κ B p65 translocation by targeting KPNA1, -2, and -4 (Taylor et

457 al., 2009). Most recently, vaccinia virus protein A55 was shown to interact with KPNA2 to disturb
458 its interaction with NF- κ B (Pallett et al., 2019). Hepatitis C virus NS3/4A protein restricts IRF3 and
459 NF- κ B translocation by cleaving KPNB1 (importin- β) (Gagne et al., 2017). We propose that the
460 different mechanisms of NF- κ B/IRF3 manipulation by different viruses reflect their reliance on
461 transcriptional activation while simultaneously depending on inhibition of the same transcription
462 factors activated by defensive processes. We hypothesise that each virus has specifically adapted
463 to manipulate nuclear transport of transcription factors to facilitate replication while dampening
464 activation of inhibitory effectors. Cell type clearly also plays a role in Vpr function. For example, in
465 monocyte derived dendritic cells, Vpr has been reported to activate NF- κ B to drive viral
466 transcription (Miller et al., 2017). A model incorporating context dependent NF- κ B activation or
467 inhibition, depending on life cycle stage and cell type, could explain apparently contradictory
468 reports that Vpr both inhibits (Ayyavoo et al., 1997; Kogan et al., 2013), but also activates NF- κ B
469 (Liu et al., 2014; Liu et al., 2013; Vermeire et al., 2016). One possibility to explain specific inhibition
470 of NF- κ B by incoming particle associated Vpr, but not Vpr expressed in the context of infection, is
471 that once the provirus is formed, and Gag is expressed, Gag recruits Vpr to viral particles to reduce
472 further manipulation of NF- κ B that is required for on-going viral transcription (Belzile et al., 2010).

473

474 Vpr has previously been shown to interact with a variety of mouse (Miyatake et al., 2016), yeast
475 (Vodicka et al., 1998) and human karyopherin proteins including human KPNA1, 2 and 5 (Nitahara-
476 Kasahara et al., 2007). Indeed, the structure of a C-terminal Vpr peptide (residues 85-96) has been
477 solved in complex with mouse importin α 2 (Miyatake et al., 2016) although this study did not shed
478 light on mechanism of innate immune manipulation by Vpr because this Vpr peptide is distant from
479 residues 34/35 shown to impact sensing (Figures 3, 5-7) and nuclear membrane localisation
480 (Figure 4). Here we confirm an interaction with KPNA1 by co-immunoprecipitation and confirm that
481 this interaction is reduced by Vpr mutation F34I/P35N (Figure 7). Critically, we demonstrate that
482 wild type Vpr, but not Vpr F34I/P35N, inhibits recruitment of IRF3 and NF- κ B explaining inhibition
483 of transcription factor nuclear entry. Failure to degrade karyopherin proteins suggests that some
484 KPNA1 nuclear import function may be left intact by the virus to facilitate a more subtle
485 manipulation of host cell biology (Figure 7). A similar model of inhibition of KPNA target binding to
486 manipulate nuclear import has been suggested by a crystal structure of Ebola Virus VP24 protein
487 in complex with KPNA5. This study proposed that VP24 targets a KPNA5 NLS binding site to
488 specifically inhibit nuclear import of phosphorylated STAT1 (Xu et al., 2014).

489

490 Our data also explain previous reports of the suppression of expression from co-transfected CMV
491 MIEP-driven plasmids by Vpr (Liu et al., 2015). Vpr inhibition of NF- κ B transport into the nucleus
492 to activate the MIEP likely explains these data, but another possibility is that transcription factor
493 bound to cytoplasmic plasmid DNA has a role in importing plasmid into the nucleus, and it is
494 plasmid transport that is inhibited (Mesika et al., 2001). Vpr insensitivity of NF- κ B-independent

495 ubiquitin and EF1 α promoters (Figure 6) is consistent with this model, summarized in Figure S7.
496 This is important because inhibition of transfected plasmid driven protein expression may explain
497 the effect of cotransfected SIV Vpr on STING and cGAS signaling reported recently (Su et al.,
498 2019). Note that STING expression was not affected by Vpr co-expression but STING was
499 expressed from the Vpr and NF- κ B-insensitive EF1 α promoter (Figure 6), whereas cGAS, which
500 was not measured by western blot, was expressed from a Vpr and NF- κ B-sensitive (Figure 6) CMV
501 driven plasmid VR1012 (Hartikka et al., 1996).

502
503 Importantly, our data are consistent with reports that manipulation of cell cycle by Vpr is
504 independent of interaction with karyopherin proteins. The Vpr R80A mutant, which does not arrest
505 cell cycle, or manipulate SLX4 complex (Gaynor & Chen, 2001; Laguette et al., 2014) was
506 functional in inhibition of innate sensing (Figures 3, 5, 6). Mapping the residues of Vpr that are
507 important for innate immune inhibition onto structures resolved by NMR and X-ray crystallography
508 reveals a potentially distinct interface from that targeting UNG2 because residues Vpr 34/35 are
509 distant from the UNG2 binding site (Figure S3B, S3C). Given that Vpr has been shown to bind
510 FxFG motif in p6 of Gag during virion incorporation (Zhu et al., 2004), and FG motifs at the NPC
511 (Fouchier et al., 1998) it is possible that interaction of Vpr with nuclear pore proteins via the FG
512 motifs contribute to Vpr mediated inhibition of IRF3 and NF- κ B nuclear import.

513
514 Our data are consistent with a model in which HIV-1 particle associated Vpr can suppress the
515 consequences of sensing (Figures 1, 3B, 5C, 6A, B). Higher amounts of activation, caused by
516 global activation of cells by externally derived PAMPs, simulated here by transfection of Poly:IC,
517 DNA treatment with LPS, or infection with Sendai virus, can also be suppressed by Vpr bearing
518 viral particles, here best evidenced by measurements of IRF3 and NF- κ B nuclear localisation
519 (Figures 5 and 6). Given that infection typically depends on exposing cells to more than one viral
520 particle, requiring 10s of particles in even the most conservative estimates, it is likely that Vpr
521 delivered by particles that do not eventually form a provirus, contributes to suppression of sensing.
522 Certainly a lower MOI is required for Vpr activity when the stimulation comes from the Vpr bearing
523 viral particles themselves, compare external stimulus (MOI 20 required, Figure 1B) and virus
524 associated stimulus (MOI 3 required, Figure 1C)

525
526 We and others, have argued that the genome of wild type HIV-1 is not efficiently sensed by nucleic
527 acid sensors, or degraded by cellular nucleases, because the capsid protects the HIV-1 genome,
528 and regulates the process of reverse transcription, during transport across a hostile cytoplasmic
529 environment, prior to uncoating at the NPC, or in the nucleus of infected cells (Bejarano et al.,
530 2019; Burdick et al., 2017; Francis et al., 2016; Jacques et al., 2016; Rasaiyaah et al., 2013;
531 Schaller et al., 2011; Sumner et al., 2019; N. Yan et al., 2010; Zila et al., 2019). Cingoz et al
532 reported failure of VSV-G pseudotyped HIV-1 (Δ Env, Δ Nef, Δ Vpr) to activate sensing in a variety

533 of cell lines (Cingöz & Goff, 2019). However, other studies have demonstrated sensing of wild type
534 HIV-1 DNA by cGAS (Gao et al., 2013; Lahaye et al., 2013), and here we observed cGAS-
535 dependent, Vpr-sensitive, induction of CXCL10 or NF- κ B reporter by high dose (MOI 3) VSV-G
536 pseudotyped single round HIV-1 GFP vector in THP-1 cells (Figure 1, 6). We assume that virus
537 dose is the most important difference between studies. Cingoz used luciferase to measure
538 infection and therefore MOIs are obscure. Note that herein, MOI calculated by GFP expression is
539 included in supplementary data for most experiments. We propose that both capsid and Vpr have
540 a role in preventing HIV-1 stimulating innate immune sensing but that Vpr can suppress stimulation
541 from external sources.

542

543 *In vitro*, primary myeloid cells behave according to the stimuli they have received. Thus,
544 inconsistent results between studies, for example the requirement here for cGAMP, but not in other
545 studies, to cause Vpr dependent replication in macrophages (Figure 1), could be explained by
546 differences in myeloid cell stimulation due to differences in cell purification and differentiation
547 methods or reagents used. Methods of virus preparation, here viruses were purified by
548 centrifugation through sucrose, may also be a source of target cell activation and experimental
549 variation. We hypothesise that cGAMP induced Vpr dependence in MDM (Figure 1) because cells
550 were not activated prior to cGAMP addition, whereas in other studies basal activation produced
551 Vpr dependent replication. Replication in activated primary CD4⁺ T cells was, in our hands,
552 independent of Vpr in the presence and absence of cGAMP, which was inhibitory, suggesting that
553 Vpr cannot overcome signalling downstream of cGAMP in these cells. This implies that activated
554 T-cells respond differently to cGAMP than macrophages, consistent observations that in T
555 cell/macrophage mixed cultures, the negative effects of cGAMP on HIV-1 replication were
556 principally mediated via macrophages (Xu et al., 2016). Vpr sensitive, cGAS dependent, IFN
557 production from T cells has been reported suggesting that in the right circumstances, T cells can
558 sense HIV-1 DNA, via cGAS, in T cells (Vermeire et al., 2016). Importantly, this study used
559 integration inhibition to demonstrate provirus-dependent detection of HIV-1 suggesting that
560 incoming HIV-1 DNA is not the cGAS target in this study. Certainly, further work is required to
561 understand the different requirements for Vpr function in T cells and macrophages.

562

563 In summary our findings connect Vpr manipulation of nuclear transport with inhibition of innate
564 immune sensing, rather than viral nuclear import. They highlight the crucial role of particle
565 associated Vpr in inhibiting innate immune activation during the early stages of the viral life cycle
566 and unify a series of studies explaining previously apparently unconnected observations. Given
567 the complexity of NF- κ B activation, and the different ways each virus manipulates defensive
568 transcriptional responses, we propose that the further study of viral inhibition of PAMP-driven
569 inflammatory responses will lead to a better understanding of the biology of the transcription factors
570 involved and highlight novel, tractable targets for therapeutic anti-inflammatory development.

571

572 **Acknowledgements**

573 We thank Veit Hornung for providing THP-1-IFIT-1 cells wild type and knock outs, Geoffrey Smith
574 for providing constructs encoding KPNA1-3 and Clare Jolly and Richard Sloan for providing
575 NL4.3ΔVpr. This work was funded through an MRC PhD studentship (HK) an MRC Clinical
576 Training Fellowship (CVT), a Wellcome Trust clinical training fellowship (DF), a Wellcome Trust
577 Senior Biomedical Research Fellowship (GJT), the European Research Council under the
578 European Union's Seventh Framework Programme (FP7/2007-2013)/ERC (grant HIVInnate
579 339223) (GJT), a Wellcome Trust Collaborative award (GJT) and was supported by the National
580 Institute for Health Research University College London Hospitals Biomedical Research Centre.

581

582 **Author contributions**

583 HK, CPT, RPS, LZA, LT, DF and GJT conceived the study. HK, RPS, JR, CPT, MTRP, CVT and
584 DS performed experiments. HK, RPS, RSBM and GJT analyzed the data. HK, RPS, RSBM and
585 GJT wrote the manuscript.

586

587 **Methods**

588

589 **Cells and reagents**

590 HEK293T cells were maintained in DMEM (Gibco) supplemented with 10 % foetal calf serum (FCS,
591 Labtech) and 100 U/ml penicillin and 100 µg/ml streptomycin (Pen/Strep; Gibco). THP-1 cells were
592 maintained in RPMI (Gibco) supplemented with 10% FCS and Pen/Strep. THP-1-IFIT-1 luciferase
593 reporter cells express Gaussia luciferase under the control of the endogenous IFIT1 promoter have
594 been described (Mankan et al., 2014). THP-1 CRISPR control, *cGAS*^{-/-} and *MAVS*^{-/-} knock out
595 cells have been described (Mankan et al., 2014). Nup358 depleted HeLa cells have been
596 described (Schaller et al., 2011). Lipopolysaccharide, poly I:C and TNF α were obtained from
597 PeproTech. Sendai virus was obtained from Charles River Laboratories. Herring-testis DNA was
598 obtained from Sigma. cGAMP was obtained from Invivogen. NF- κ B Lucia THP-1 reporter cells
599 were obtained from Invivogen.

600

601 **Cloning and plasmids**

602 The Vpr gene from HIV-1 founder clone SUMA (Fischer et al., 2010) was codon optimised and
603 synthesised by GeneArt. To generate the HIV-1 vector encoding Vpr (pCSVIG), the codon
604 optimised SUMA Vpr gene was cloned into pSIN-BX-IRES-Em between BamHI and XhoI sites
605 under the control of the SFFV LTR promoter. pSIN-BX-IRES-Em was obtained from Dr Yasuhiro
606 Takeuchi. EF1 α -GFP and UB-GFP were obtained from Addgene (Matsuda & Cepko, 2004). The
607 CMV-GFP construct was pEGFPC1 (Clontech). HIV-1 bearing a Ba-L envelope gene has been
608 described (Rasaiyaah et al., 2013). Flag- KPNA1-3 plasmids were obtained from Prof. Geoffrey

609 Smith. HIV-1 Δ Vpr was a gift from Richard Sloan and encoded an 17 nucleotide insertion (Vpr 64-
610 81) that destroys the Vpr coding sequence.

611

612 **Production of virus in HEK293T cells**

613 Replication competent HIV-1 and VSV-G pseudotyped HIV-1 GFP vectors were produced by
614 transfection of HEK293T cells in T150 flasks using Fugene 6 transfection reagent (Promega)
615 according to the manufacturer's instructions. Briefly, just-subconfluent T150 flasks were
616 transfected with 8.75 μ g of HIV-1 YU2 or HIV-1 YU2 lacking Vpr (HIV-1 YU2 Δ Vpr) and 30 μ l
617 Fugene 6 in 500 μ l Optimem (Thermofisher Scientific). To make VSV-G pseudotyped HIV-1 GFP,
618 each T150 flask was transfected with 2.5 μ g of vesicular stomatitis virus-G glycoprotein encoding
619 plasmid (pMDG) (Genscript), 2.5 μ g of packaging plasmid, p8.91 (encoding Gag-Pol, Tat and Rev)
620 or p8.2 (encoding Gag-Pol, Tat and Rev and Vif, Vpr, Vpu and Nef) (Zufferey et al., 1997), and
621 3.75 μ g of GFP encoding genome plasmid (pCSGW) using 30 μ l Fugene 6 in 500 μ l optimum. To
622 make Vpr encoding HIV-1 GFP, 3.75 μ g pCSVIG was transfected with 2.5 μ g of pMDG and 2.5 μ g
623 of p8.91. To make HIV-1 GFP particles bearing Vpr, 1 μ g of Vpr expressing pcDNA3.1 (wild type
624 SUMA Vpr or Vpr mutants) was transfected with 2.5 μ g of pMDG and 2.5 μ g of p8.91 in 30 μ l
625 Fugene-6 and 500 μ l Optimem. All virus supernatants were harvested at 48 and 72 h post-
626 transfection, replicate flasks were pooled, and supernatants subjected to ultracentrifugation
627 through a 20% sucrose cushion at 23000 rpm for 2 hours in a 30 ml swingout rotor (Sorvall)
628 (72000G). Viral particles were resuspended in RPMI supplemented with 10% FCS. HIV-GFP
629 produced with p8.91 or p8.2 used in Figure 1 were DNase treated for 2 hours at 37°C (DNaseI,
630 Sigma) prior to ultracentrifugation. Viruses were titrated by infecting THP-1 cells (2×10^5 cells/ml)
631 with dilutions of sucrose purified virus in the presence of polybrene (8 μ g/ml, Sigma) and incubating
632 for 48 h. GFP-positive, infected cells were counted by flow cytometry using a BD Accuri C6
633 (BDBiosciences). HIV-1 vector encoding shRNA targeting DCAF1 has been described and was
634 prepared as above (Berger et al., 2015).

635

636 **SG-PERT**

637 Viral doses were determined by measuring reverse transcriptase activity of virus preparations by
638 qPCR using a SYBR Green-based product-enhanced PCR assay (SG-PERT) as described (Jolien
639 Vermeire et al., 2012).

640

641 **Isolation of primary monocyte-derived macrophages and CD4⁺ T cells from peripheral** 642 **blood**

643 Primary monocyte-derived macrophages (MDM) were prepared from fresh blood from healthy
644 volunteers. The study was approved by the joint University College London/University College
645 London Hospitals NHS Trust Human Research Ethics Committee. Primary CD4⁺ T cells were
646 obtained from leukocyte cones from healthy donors. Peripheral blood mononuclear cells (PBMCs)

647 were isolated by density gradient centrifugation using Lymphoprep (Stemcell Technologies). For
648 MDM preparation, PBMCs were washed three times with PBS and plated to select for adherent
649 cells. Non-adherent cells were washed away after 1.5 h and the remaining cells incubated in RPMI
650 (Gibco) supplemented with 10 % heat-inactivated pooled human serum (Sigma) and 40 ng/ml
651 macrophage colony stimulating factor (R&D systems). Cells were further washed after 3 days and
652 the medium changed to RPMI supplemented with 10% heat-inactivated human serum (Sigma).
653 MDM were then infected 3-4 days later at low multiplicity of infection. Spreading infection was
654 detected by Gag staining and counting Gag positive cells as described (Rasaiyaah et al., 2013).
655 For CD4+ T cells, untouched CD4+ T cells were purified from PBMCs with an indirect magnetic
656 labeling system (MACS, Miltenyi Biotec), according to manufacturer's instructions. Cells were then
657 cultured with 2 µg/ml of plate-bound anti-CD3 and anti-CD28 monoclonal antibodies (αCD3αCD28
658 stimulation) (mAbs) (eBioscience) and 25 U/ml of recombinant human interleukin-2 (IL-2; Roche
659 Applied Science) at a concentration of 1.5-2 x 10⁶ cells/ml in RPMI supplemented with 10% heat-
660 inactivated Human Serum (HS) (SigmaAldrich). Cells were maintained at 37°C in 5% CO₂ in a
661 humidified incubator for 72 h. CD4+ T cells were then assessed for spreading infection of CXCR4-
662 tropic HIV-1 NL4.3 WT and ΔVPR at low multiplicity of infection (300 mU of HIV-1 RT Activity per
663 1x10⁶ cells). Percentage of HIV-1-infected primary CD4+ T cells was determined by flow cytometry
664 measuring p24Gag antigen employing the monoclonal antibody p24Gag-FITC (HIV-1 p24 (24-4),
665 Santa Cruz Biotechnology).

666

667 **Innate immune sensing assays**

668 THP-1 cells were seeded in 96 well plates (5x10⁵ cells/ml). For Vpr expression, cells were infected
669 with an empty or Vpr expressing (pCSVIG) lentiviral vectors for 40 hours. For stimulation of cells
670 with HT-DNA or poly I:C, 0.2 µl of lipofectamine and 25 µl of Optimem were incubated with HT-
671 DNA or poly I:C (amounts stated in figure legends) for 20 minutes and added to cells.
672 Lipopolysaccharide (1 µg/ml), TNFα (200 ng/ml), Sendai virus (200 HA U/ml) or cGAMP (5 µg/ml)
673 were added directly to the media. For experiments with virion delivered/associated Vpr, cells were
674 stimulated at the time of infection. Gaussia/Luciferase activities were measured 8 hours post
675 cell stimulation/infection by transferring 10 µl supernatant to a white 96 well assay plate, injecting
676 50 µl per well of coelenterazine substrate (Nanolight Technologies, 2 µg/ml) and analysing
677 luminescence on a FLUOstar OPTIMA luminometer (Promega). Data were normalized to a mock-
678 treated control to generate a fold induction.

679

680 **ELISA**

681 Cell supernatants were harvested for ELISA at 8 h post-stimulation and stored at -80 °C. CXCL-
682 10 protein was measured using Duoset ELISA reagents (R&D Biosystems) according to the
683 manufacturer's instructions.

684

685 **ISG qPCR**

686 RNA was extracted from THP-1 cells using a total RNA purification kit (Norgen) according to the
687 manufacturer's protocol. Five hundred ng RNA was used to synthesise cDNA using Superscript III
688 reverse transcriptase (Invitrogen), also according to the manufacturer's protocol. cDNA was diluted
689 1:5 in water and 2 μ l was used as a template for real-time PCR using SYBR® Green PCR master
690 mix (Applied Biosystems) and a 7900HT Real-Time PCR machine (Applied Biosystems).
691 Expression of each gene was normalised to an internal control (*GAPDH*) and these values were
692 then normalised to mock-treated control cells to yield a fold induction. The following primers were
693 used:

694 *GAPDH*: Fwd 5'-GGGAACTGTGGCGTGAT-3', Rev 5'-GGAGGAGTGGGTGTCGCTGTT-3'

695 *CXCL-10*: Fwd 5'-TGGCATTCAAGGAGTACCTC-3', Rev 5'-TTGTAGCAATGATCTCAACACG-3'

696 *IFIT-2*: Fwd 5'-CAGCTGAGAATTGCACTGCAA-3', Rev 5'-CGTAGGCTGCTCTCCAAGGA-3'

697 *MxA*: Fwd 5'-ATCCTGGGATTTTGGGGCTT-3', Rev 5'-CCGCTTGTGCTGGTGTGCG-3'

698 *Viperin*: Fwd 5'-CTGTCCGCTGGAAAGTG-3', Rev 5'-GCTTCTTCTACACCAACATCC-3'

699 *IL-6*: Fwd 5'- AAATTCGGTACATCCTCGACG-3', Rev 5'- GGAAGGTTTCAGGTTGTTTTCT-3'

700

701 **Immunofluorescence**

702 For confocal microscopy, HeLa cells (5×10^4 cells/ml) were seeded into 24-well plates containing
703 sterile glass coverslips. For nuclear translocation assays, we used THP-1 cells (4×10^5 cells/ml)
704 adhered in an optical 96-well plate (PerkinElmer) with 50 ng/ml phorbol 12-myristate 13-acetate
705 (PMA, Peprotech) for 48 hours. Where cells were infected and transfected (DNA, PolyI:C) or
706 treated (cGAMP) with innate immune stimulants, the cells were treated or transfected first, and
707 then viral supernatant added to the cultures. Cells were then fixed and stained three hours after
708 this. For fixation, HeLa or adhered THP-1 cells were washed twice with ice-cold PBS and fixed in
709 4% (vol/vol) paraformaldehyde. Autofluorescence was quenched in 150 mM ammonium chloride,
710 the cells permeabilized in 0.1% (vol/vol) Triton X-100 in PBS and blocked for 30 min in 5% (vol/vol)
711 FCS in PBS. Cells were incubated with primary Ab for 1 hour followed by incubation with secondary
712 Ab for 1 hour. Cells were washed with PBS three times between each step. The coverslips were
713 placed on a slide prepared with a 30 μ l drop of mounting medium (Vectashield, containing 4',6-
714 diamidino-2-phenylindole (DAPI)) and allowed to set before storing at 4° C. Images were taken on
715 a Leica TCS SPE confocal microscope and analyzed in ImageJ. For IRF3/NF- κ B(p65)
716 translocation, images were taken on Hermes WISCAN (IDEA Bio-Medical) and analyzed with
717 Metamorph software (Molecular Devices). Metamorph calculated a translocation coefficient
718 representing the proportion of staining in nuclear versus cytoplasmic compartments. A value of 1
719 represents "all staining in the nucleus", -1 is "exclusively in cytoplasm" and 0 is "equally
720 distributed".

721

722 Primary antibodies were from the following sources: Mouse-anti-FXFG repeats containing

723 nucleoporins (Mab414) (Abcam), Rabbit-anti-flag (Sigma), Rabbit-anti-IRF3 (Santa Cruz
724 Biotechnology) and Mouse-anti-NF- κ B p65 (Santa Cruz Biotechnology). Primary antibodies were
725 detected with Goat-anti-rabbit Alexa Fluor 488 IgG (Invitrogen) or Goat-anti-mouse Alexa Fluor
726 546 IgG (Invitrogen).

727

728 **Immunoblotting**

729 For immunoblotting of viral particles, sucrose purified (as described above) virions (1×10^{11} RT
730 units) were boiled for 10 min in 6X Laemmli buffer (50 mM Tris-HCl (pH 6.8), 2 % (w/v) SDS, 10%
731 (v/v) glycerol, 0.1% (w/v) bromophenol blue, 100 mM β -mercaptoethanol) before separating on 12
732 % polyacrylamide gel. Cells were lysed in lysis buffer containing 50 mM Tris pH 8, 150 mM NaCl,
733 1 mM EDTA, 10% (v/v) glycerol, 1 % (v/v) Triton X100, 0.05 % (v/v) NP40 supplemented with
734 protease inhibitors (Roche), clarified by centrifugation at 14,000 x g for 10 min and boiled in 6X
735 Laemmli buffer for 10 min. Proteins were separated by SDS-PAGE on 12% polyacrylamide gels.
736 Proteins were transferred to a Hybond ECL membrane (Amersham biosciences) using a semi-dry
737 transfer system (Biorad). Primary antibodies were from the following sources: Rabbit-anti-VSV-G
738 (Sigma), Rabbit-anti-HIV-1 p24 (NIH AIDS reagent program), Rabbit-anti-STING (Cell signaling),
739 Rabbit-anti-pSTING (Cell signaling), Rabbit-anti-TBK1 (Cell signaling), Rabbit-anti-pTBK1 (Cell
740 signaling), Rabbit-anti-IRF3 (Cell signaling), Rabbit-anti-pIRF3-386 (Sigma), Mouse-anti-actin
741 (Abcam), Rabbit-anti-cGAS (Cell Signaling Technology), Mouse-anti-MAVS (Cell Signaling
742 Technology), Rabbit-anti-DCAF1 (Bethyl), Rabbit-anti-Nup358 (Abcam), Mouse-anti-flag (Sigma),
743 Rabbit-anti-GFP (Abcam), KPNA1-6 (ABclonal), KPNB1 (ABclonal), Rabbit-anti-cypB (Abcam),
744 Mouse-anti-FLAG (Sigma), Rabbit-anti-HA (Sigma) and Rabbit-anti-Vpr (NIH). Primary antibodies
745 were detected with goat-anti-mouse/rabbit IRdye 800CW infrared dye secondary antibodies and
746 membranes imaged using an Odyssey Infrared Imager (LI-COR Biosciences).

747

748 **Cell cycle analysis**

749 WT Vpr or Vpr mutants were expressed in THP-1 cells using pCSVIG at an MOI of 1. Cells were
750 incubated for 48 hours and then washed with PBS and fixed in 1 ml cold 70% ethanol on ice for
751 30 minutes. To ensure efficient fixing and minimise clumping, ethanol was added dropwise while
752 vortexing. Cell were pelleted in a microfuge and ethanol was removed followed by two wash steps
753 with PBS. To remove RNA from the samples, RNase A (100 μ g/ml) was added and the cells were
754 stained with propidium iodide (PI) (50 μ g/ml) to stain cellular DNA. Cells were incubated for 10
755 minutes at room temperature and DNA content analysed by flow cytometry on a BD FACSCalibur
756 (BD Biosciences). The data were analysed with FlowJo.

757

758 **Generation of Vpr mutants**

759 Site directed mutagenesis was performed using Pfu Turbo DNA Polymerase (Agilent) according
760 to the manufacturer's instructions with the following primers using either pCDNA3.1 or pCSVIG
761 encoding SUMA Vpr as template.

762 VprF34I+P35N: Fwd 5'-GCCGTGCGGCACATCAACAGACCTTGGCTGCATAGC-3',

763 Rev 5'-GCTATGCAGCCAAGGTCTGTTGATGTGCCGCACGGC-3'

764 VprQ65R: Fwd 5'-GCCATCATCAGAATCCTGCGGCAGCTGCTGTTTCATC-3',

765 Rev 5'-GATGAACAGCAGCTGCCGCAGGATTCTGATGATGGC-3'

766 VprR80A: Fwd 5'-GGCTGCCGGCACAGCGCCATCGGCATCACCCCT-3',

767 Rev 5'-AGGGGTGATGCCGATGGCGCTGTGCCGGCAGCC-3'

768

769 **Co-immunoprecipitation assays**

770 HEK293T cells were grown in 10 cm dishes and co-transfected with plasmids expressing a FLAG-
771 tagged protein (1 µg KPNA1, KPNA2, KPNA3, GFP or empty vector (EV)) and 1 µg of a plasmid
772 expressing HA-tagged SUMA Vpr wild-type, or Vpr F34I/P35N mutant using 6 µl Fugene-6
773 (Promega). For KPNA-cargo IPs HEK293T cells were grown in 10 cm dishes and co-transfected
774 with 1 µg of a plasmid expressing FLAG-tagged KPNA1, 1 µg of a plasmid expressing HA-tagged
775 p65 or IRF3 and 1 µg of a plasmid expressing un-tagged Vpr, VprF34I+P35N or empty vector
776 control. After 24 h cells were lysed in lysis buffer (0.5 (v/v) % NP-40 in PBS supplemented with
777 protease inhibitors (Roche) and phosphatase inhibitors (Roche), pre-cleared by centrifugation and
778 incubated with 25 µl of mouse-anti-HA agarose beads (Millipore) or mouse-anti-FLAG M2 agarose
779 affinity gel (Sigma) for 2-4 h. Immunoprecipitates were washed 3 times in 1 ml of lysis buffer and
780 eluted from the beads by boiling in 20 µl of 2X sample buffer containing SDS and β-
781 mercaptoethanol. Proteins were resolved by SDS-polyacrylamide gel electrophoresis (NuPAGE 4-
782 12 % Bis-Tris protein gels, Invitrogen) and detected by immunoblotting.

783

784 **Statistical analyses**

785 Data were analysed by statistical tests as indicated in the figure legends. * represent statistical
786 significance: * (p<0.05), ** (p<0.01), *** (p<0.001), **** (p<0.0001).

787

788 **References**

789

790 Ali, A., Ng, H. L., Blankson, J. N., Burton, D. R., Buckheit, R. W. 3rd, Moldt, B., Fulcher, J. A.,

791 Ibarrondo, F. J., Anton, P. A., & Yang, O. O. (2018). Highly Attenuated Infection With a Vpr-

792 Deleted Molecular Clone of Human Immunodeficiency Virus-1. *The Journal of Infectious*

793 *Diseases*, 218(9), 1447–1452. <https://doi.org/10.1093/infdis/jiy346>

794 Andrejeva, J., Childs, K. S., Young, D. F., Carlos, T. S., Stock, N., Goodbourn, S., & Randall, R. E.

795 (2004). The V proteins of paramyxoviruses bind the IFN-inducible RNA helicase, mda-5, and

796 inhibit its activation of the IFN-β promoter. *Proceedings of the National Academy of Sciences of*

797 *the United States of America*, 101(49), 17264–17269. <https://doi.org/10.1073/pnas.0407639101>

- 798 Ayyavoo, V., Mahboubi, A., Mahalingam, S., Ramalingam, R., Kudchodkar, S., Williams, W. V., Green,
799 D. R., & Weiner, D. B. (1997). HIV-1 Vpr suppresses immune activation and apoptosis through
800 regulation of nuclear factor kappa B. *Nature Medicine*, 3(10), 1117–1123.
801 <https://doi.org/10.1038/nm1097-1117>
- 802 Bachand, F., Yao, X.-J., Hrimech, M., Rougeau, N., & Cohen, É. A. (1999). Incorporation of Vpr into
803 human immunodeficiency virus type 1 requires a direct interaction with the p6 domain of the p55
804 Gag precursor. *Journal of Biological Chemistry*, 274(13), 9083–9091.
805 <https://doi.org/10.1074/jbc.274.13.9083>
- 806 Bejarano, D. A., Peng, K., Laketa, V., Börner, K., Jost, K. L., Lucic, B., Glass, B., Lusic, M., Müller, B.,
807 & Kräusslich, H.-G. (2019). HIV-1 nuclear import in macrophages is regulated by CPSF6-capsid
808 interactions at the nuclear pore complex. *ELife*, 8, e41800. <https://doi.org/10.7554/elife.41800>
- 809 Belzile, J. P., Abrahamyan, L. G., Gérard, F. C. A., Rougeau, N., & Cohen, É. A. (2010). Formation of
810 mobile chromatin-associated nuclear foci containing HIV-1 Vpr and VPRBP is critical for the
811 induction of G2 cell cycle arrest. *PLoS Pathogens*, 6(9), e1001080.
812 <https://doi.org/10.1371/journal.ppat.1001080>
- 813 Berger, G., Lawrence, M., Hué, S., & Neil, S. J. D. (2015). G2/M cell cycle arrest correlates with
814 primate lentiviral Vpr interaction with the SLX4 complex. *Journal of Virology*, 89(1), 230–240.
815 <https://doi.org/10.1128/JVI.02307-14>
- 816 Burdick, R. C., Delviks-Frankenberry, K. A., Chen, J., Janaka, S. K., Sastri, J., Hu, W. S., & Pathak,
817 V. K. (2017). Dynamics and regulation of nuclear import and nuclear movements of HIV-1
818 complexes. *PLoS Pathogens*, 13(8), e1006570. <https://doi.org/10.1371/journal.ppat.1006570>
- 819 Chen, W., Srinath, H., Lam, S. S., Schiffer, C. A., Royer, W. E., & Lin, K. (2008). Contribution of
820 Ser386 and Ser396 to Activation of Interferon Regulatory Factor 3. *Journal of Molecular Biology*,
821 379(2), 251–260. <https://doi.org/10.1016/j.jmb.2008.03.050>
- 822 Cingöz, O., & Goff, S. P. (2019). HIV-1 Is a Poor Inducer of Innate Immune Responses. *MBio*, 10(1),
823 e02834-18. <https://doi.org/10.1128/mBio.02834-18>
- 824 Connor, R. I., Chen, B. K., Choe, S., & Landau, N. R. (1995). Vpr is required for efficient replication of
825 human immunodeficiency virus type-1 in mononuclear phagocytes. *Virology*, 206(2), 935–944.
826 <https://doi.org/10.1006/viro.1995.1016>
- 827 de Queiroz, N. M. G. P., Xia, T., Konno, H., & Barber, G. N. (2019). Ovarian Cancer Cells Commonly
828 Exhibit Defective STING Signaling Which Affects Sensitivity to Viral Oncolysis. *Molecular*
829 *Cancer Research : MCR*, 17(4), 974–986. <https://doi.org/10.1158/1541-7786.MCR-18-0504>
- 830 Dedera, D., Hu, W., Vander, N., Heyden, & Ran, L. (1989). Viral Protein R of Human
831 Immunodeficiency Virus Types 1 and 2 Is Despensable for Replication and Cytopathogenicity in
832 Lymphoid Cells. *Journal of Virology*, 63(7), 3205–3208. <https://doi.org/10.1007/BF02297789>
- 833 DeMeritt, I. B., Milford, L. E., & Yurochko, A. D. (2004). Activation of the NF- κ B Pathway in Human
834 Cytomegalovirus-Infected Cells Is Necessary for Efficient Transactivation of the Major
835 Immediate-Early Promoter. *Journal of Virology*, 78(9), 498–507.
836 <https://doi.org/10.1128/jvi.78.9.4498-4507.2004>
- 837 Fagerlund, R., Kinnunen, L., Kohler, M., Julkunen, I., & Melen, K. (2005). NF- κ B is transported

- 838 into the nucleus by importin {alpha}3 and importin {alpha}4. *The Journal of Biological Chemistry*,
839 280(16), 15942–15951. <https://doi.org/10.1074/jbc.M500814200>
- 840 Fagerlund, R., Melén, K., Cao, X., & Julkunen, I. (2008). NF- κ B p52, RelB and c-Rel are transported
841 into the nucleus via a subset of importin α molecules. *Cellular Signalling*, 20(8), 1442–1451.
842 <https://doi.org/10.1016/j.cellsig.2008.03.012>
- 843 Fang, R., Wang, C., Jiang, Q., Lv, M., Gao, P., Yu, X., Mu, P., Zhang, R., Bi, S., Feng, J.-M., & Jiang,
844 Z. (2017). NEMO–IKK β Are Essential for IRF3 and NF- κ B Activation in the cGAS–STING
845 Pathway. *The Journal of Immunology*, 199(9), 3222–3233.
846 <https://doi.org/10.4049/jimmunol.1700699>
- 847 Fischer, W., Ganusov, V. V., Giorgi, E. E., Hraber, P. T., Keele, B. F., Leitner, T., Han, C. S.,
848 Gleasner, C. D., Green, L., Lo, C.-C., Nag, A., Wallstrom, T. C., Wang, S., McMichael, A. J.,
849 Haynes, B. F., Hahn, B. H., Perelson, A. S., Borrow, P., Shaw, G. M., ... Korber, B. T. (2010).
850 Transmission of single HIV-1 genomes and dynamics of early immune escape revealed by ultra-
851 deep sequencing. *PloS One*, 5(8), e12303–e12303.
852 <https://doi.org/10.1371/journal.pone.0012303>
- 853 Foster, T L, Wilson, H., Iyer, S. S., Coss, K., Doores, K., Smith, S., Kellam, P., Finzi, A., Borrow, P.,
854 Hahn, B. H., & Neil, S. J. D. (2016). Resistance of Transmitted Founder HIV-1 to IFITM-
855 Mediated Restriction. *Cell Host and Microbe*, 20(4), 429–442.
856 <https://doi.org/10.1016/j.chom.2016.08.006>
- 857 Foster, Toshana L, Pickering, S., & Neil, S. J. D. (2017). Inhibiting the Ins and Outs of HIV
858 Replication: Cell-Intrinsic Antiretroviral Restrictions at the Plasma Membrane. *Frontiers in*
859 *Immunology*, 8, 1853. <https://doi.org/10.3389/fimmu.2017.01853>
- 860 Fouchier, R. A. M., Meyer, B. E., Simon, J. H. M., Fischer, U., Albright, A. V, González-Scarano, F., &
861 Malim, M. H. (1998). Interaction of the human immunodeficiency virus type 1 Vpr protein with the
862 nuclear pore complex. *Journal of Virology*, 72(7), 6004–6013.
863 [https://www.scopus.com/inward/record.uri?eid=2-s2.0-
864 0031799691&partnerID=40&md5=95c739e3621c2e60756318f4b498b0e9](https://www.scopus.com/inward/record.uri?eid=2-s2.0-0031799691&partnerID=40&md5=95c739e3621c2e60756318f4b498b0e9)
- 865 Francis, A. C., Marin, M., Shi, J., Aiken, C., & Melikyan, G. B. (2016). Time-Resolved Imaging of
866 Single HIV-1 Uncoating In Vitro and in Living Cells. *PLoS Pathogens*, 12(6), e1005709.
867 <https://doi.org/10.1371/journal.ppat.1005709>
- 868 Gagne, B., Tremblay, N., Park, A. Y., Baril, M., & Lamarre, D. (2017). Importin beta1 targeting by
869 hepatitis C virus NS3/4A protein restricts IRF3 and NF-kappaB signaling of IFNB1 antiviral
870 response. *Traffic (Copenhagen, Denmark)*, 18(6), 362–377. <https://doi.org/10.1111/tra.12480>
- 871 Gao, D., Wu, J., Wu, Y.-T., Du, F., Aroh, C., Yan, N., Sun, L., & Chen, Z. J. (2013). Cyclic GMP-AMP
872 synthase is an innate immune sensor of HIV and other retroviruses. *Science*, 341(6148), 903–
873 906. <https://doi.org/10.1126/science.1240933>
- 874 Gaynor, E. M., & Chen, I. S. Y. (2001). Analysis of apoptosis induced by HIV-1 Vpr and examination
875 of the possible role of the hHR23A protein. *Experimental Cell Research*, 267(2), 243–257.
876 <https://doi.org/10.1006/excr.2001.5247>
- 877 Goujon, C., Moncorgé, O., Bauby, H., Doyle, T., Ward, C. C., Schaller, T., Hué, S., Barclay, W. S.,

- 878 Schulz, R., & Malim, M. H. (2013). Human MX2 is an interferon-induced post-entry inhibitor of
879 HIV-1 infection. *Nature*, *502*(7472), 559–562. <https://doi.org/10.1038/nature12542>
- 880 Greenwood, E. J. D., Williamson, J. C., Sienkiewicz, A., Naamati, A., Matheson, N. J., & Lehner, P. J.
881 (2019). Promiscuous Targeting of Cellular Proteins by Vpr Drives Systems-Level Proteomic
882 Remodeling in HIV-1 Infection. *Cell Reports*, *27*(5), 1579-1596.e7.
883 <https://doi.org/10.1016/j.celrep.2019.04.025>
- 884 Gulen, M. F., Koch, U., Haag, S. M., Schuler, F., Apetoh, L., Villunger, A., Radtke, F., & Ablasser, A.
885 (2017). Signalling strength determines proapoptotic functions of STING. *Nature*
886 *Communications*. <https://doi.org/10.1038/s41467-017-00573-w>
- 887 Harman, A. N., Nasr, N., Feetham, A., Galoyan, A., Alshehri, A. A., Rambukwelle, D., Botting, R. A.,
888 Hiener, B. M., Diefenbach, E., Diefenbach, R. J., Kim, M., Mansell, A., & Cunningham, A. L.
889 (2015). HIV Blocks Interferon Induction in Human Dendritic Cells and Macrophages by
890 Dysregulation of TBK1. *Journal of Virology*, *89*(13), 6575–6584.
891 <https://doi.org/10.1128/jvi.00889-15>
- 892 Hartikka, J., Sawdey, M., Cornefert-Jensen, F., Margalith, M., Barnhart, K., Nolasco, M., Vahlsing, H.
893 L., Meek, J., Marquet, M., Hobart, P., Norman, J., & Manthorpe, M. (1996). An improved plasmid
894 DNA expression vector for direct injection into skeletal muscle. *Human Gene Therapy*, *7*(10),
895 1205–1217. <https://doi.org/10.1089/hum.1996.7.10-1205>
- 896 Hattori, N., Michaels, F., Fargnoli, K., Marcon, L., Gallo, R. C., & Franchini, G. (1990). The human
897 immunodeficiency virus type 2 vpr gene is essential for productive infection of human
898 macrophages. *Proceedings of the National Academy of Sciences*, *87*(20), 8080–8084.
899 <https://doi.org/10.1073/pnas.87.20.8080>
- 900 Heiber, J. F., & Barber, G. N. (2012). Evaluation of innate immune signaling pathways in transformed
901 cells. *Methods in Molecular Biology (Clifton, N.J.)*, *797*, 217–238. https://doi.org/10.1007/978-1-61779-340-0_15
- 903 Heinzinger, N. K., Bukrinsky, M. I., Haggerty, S. A., Ragland, A. M., Kewalramani, V., Lee, M.-A.,
904 Gendelman, H. E., Ratner, L., Stevenson, M., & Emerman, M. (1994). The Vpr protein of human
905 immunodeficiency virus type 1 influences nuclear localization of viral nucleic acids in nondividing
906 host cells. *Proceedings of the National Academy of Sciences of the United States of America*,
907 *91*(15), 7311–7315. <https://doi.org/10.1073/pnas.91.15.7311>
- 908 Iyer, S. S., Bibollet-Ruche, F., Sherrill-Mix, S., Learn, G. H., Plenderleith, L., Smith, A. G., Barbian, H.
909 J., Russell, R. M., Gondim, M. V. P., Bahari, C. Y., Shaw, C. M., Li, Y., Decker, T., Haynes, B.
910 F., Shaw, G. M., Sharp, P. M., Borrow, P., & Hahn, B. H. (2017). Resistance to type 1
911 interferons is a major determinant of HIV-1 transmission fitness. *Proceedings of the National*
912 *Academy of Sciences of the United States of America*, *114*(4), E590–E599.
913 <https://doi.org/10.1073/pnas.1620144114>
- 914 Jacques, D. A., McEwan, W. A., Hilditch, L., Price, A. J., Towers, G. J., & James, L. C. (2016). HIV-1
915 uses dynamic capsid pores to import nucleotides and fuel encapsidated DNA synthesis. *Nature*,
916 *536*(7616), 349–353. <https://doi.org/10.1038/nature19098>
- 917 Jacquot, G, Le Rouzic, E., David, A., Mazzolini, J., Bouchet, J., Bouaziz, S., Niedergang, F., Pancino,

- 918 G., & Benichou, S. (2007). Localization of HIV-1 Vpr to the nuclear envelope: Impact on Vpr
919 functions and virus replication in macrophages. *Retrovirology*, 4(84), 123–176.
920 <https://doi.org/10.1186/1742-4690-4-84>
- 921 Jacquot, Guillaume, Le Rouzic, E., David, A., Mazzolini, J., Bouchet, J., Bouaziz, S., Niedergang, F.,
922 Pancino, G., & Benichou, S. (2007). Localization of HIV-1 Vpr to the nuclear envelope: Impact
923 on Vpr functions and virus replication in macrophages. *Retrovirology*, 4(84), 123–176.
924 <https://doi.org/10.1186/1742-4690-4-84>
- 925 Jimenez-Guardeño, J. M., Apolonia, L., Betancor, G., & Malim, M. H. (2019). Immunoproteasome
926 activation enables human TRIM5 α restriction of HIV-1. *Nature Microbiology*, 4(6), 933–940.
927 <https://doi.org/10.1038/s41564-019-0402-0>
- 928 Kane, M., Yadav, S. S., Bitzegeio, J., Kutluay, S. B., Zang, T., Wilson, S. J., Schoggins, J. W., Rice,
929 C. M., Yamashita, M., Hatzioannou, T., & Bieniasz, P. D. (2013). MX2 is an interferon-induced
930 inhibitor of HIV-1 infection. *Nature*, 502(7472), 563–566. <https://doi.org/10.1038/nature12653>
- 931 Kogan, M., Deshmane, S., Sawaya, B. E., Gracely, E. J., Khalili, K., & Rappaport, J. (2013). Inhibition
932 of NF- κ B activity by HIV-1 Vpr is dependent on Vpr binding protein. *Journal of Cellular*
933 *Physiology*, 228(4), 781–790. <https://doi.org/10.1002/jcp.24226>
- 934 Kumar, K. P., McBride, K. M., Weaver, B. K., Dingwall, C., & Reich, N. C. (2002). Regulated Nuclear-
935 Cytoplasmic Localization of Interferon Regulatory Factor 3, a Subunit of Double-Stranded RNA-
936 Activated Factor 1. *Molecular and Cellular Biology*, 20(11), 4159–4168.
937 <https://doi.org/10.1128/mcb.20.11.4159-4168.2000>
- 938 Laguette, N., Brégnard, C., Hue, P., Basbous, J., Yatim, A., Larroque, M., Kirchhoff, F., Constantinou,
939 A., Sobhian, B., & Benkirane, M. (2014). Premature activation of the slx4 complex by vpr
940 promotes g2/m arrest and escape from innate immune sensing. *Cell*, 156(1–2), 134–145.
941 <https://doi.org/10.1016/j.cell.2013.12.011>
- 942 Lahaye, X., Satoh, T., Gentili, M., Cerboni, S., Conrad, C., Hurbain, I., ElMarjou, A., Lacabaratz, C.,
943 Lelièvre, J.-D., & Manel, N. (2013). The Capsids of HIV-1 and HIV-2 Determine Immune
944 Detection of the Viral cDNA by the Innate Sensor cGAS in Dendritic Cells. *Immunity*, 39(6),
945 1132–1142. <https://doi.org/10.1016/j.immuni.2013.11.002>
- 946 Lahouassa, H., Blondot, M.-L., Chauveau, L., Chougui, G., Morel, M., Leduc, M., Guillonneau, F.,
947 Ramirez, B. C., Schwartz, O., & Margottin-Goguet, F. (2016). HIV-1 Vpr degrades the HLTF
948 DNA translocase in T cells and macrophages. *Proceedings of the National Academy of*
949 *Sciences of the United States of America*, 113(19), 5311–5316.
950 <https://doi.org/10.1073/pnas.1600485113>
- 951 Le Rouzic, E., Mousnier, A., Rustum, C., Stutz, F., Hallberg, E., Dargemont, C., & Benichou, S.
952 (2002). Docking of HIV-1 vpr to the nuclear envelope is mediated by the interaction with the
953 nucleoporin hCG1. *Journal of Biological Chemistry*, 277(47), 45091–45098.
954 <https://doi.org/10.1074/jbc.M207439200>
- 955 Liang, P., Zhang, H., Wang, G., Li, S., Cong, S., Luo, Y., & Zhang, B. (2013). KPNB1, XPO7 and
956 IPO8 mediate the translocation of NF- κ B/p65 into the nucleus. *Traffic (Copenhagen,*
957 *Denmark)*, 14(11), 1132–1143. <https://doi.org/10.1111/tra.12097>

- 958 Lin, R., Mamane, Y., & Hiscott, J. (1999). Structural and functional analysis of interferon regulatory
959 factor 3: localization of the transactivation and autoinhibitory domains. *Molecular and Cellular*
960 *Biology*, 19(4), 2465–2474.
- 961 Liu, R, Lin, Y., Jia, R., Geng, Y., Liang, C., Tan, J., & Qiao, W. (2014). HIV-1 Vpr stimulates NF- κ B
962 and AP-1 signaling by activating TAK1. *Retrovirology*, 11(1). [https://doi.org/10.1186/1742-4690-](https://doi.org/10.1186/1742-4690-11-45)
963 11-45
- 964 Liu, Ruikang, Tan, J., Lin, Y., Jia, R., Yang, W., Liang, C., Geng, Y., & Qiao, W. (2013). HIV-1 Vpr
965 activates both canonical and noncanonical NF- κ B pathway by enhancing the phosphorylation of
966 IKK α /B. *Virology*. <https://doi.org/10.1016/j.virol.2013.01.020>
- 967 Liu, S., Cai, X., Wu, J., Cong, Q., Chen, X., Li, T., Du, F., Ren, J., Wu, Y. T., Grishin, N. V., & Chen,
968 Z. J. (2015). Phosphorylation of innate immune adaptor proteins MAVS, STING, and TRIF
969 induces IRF3 activation. *Science*, 13(347), 2630. <https://doi.org/10.1126/science.aaa2630>
- 970 Liu, X., Guo, H., Wang, H., Markham, R., Wei, W., & Yu, X. F. (2015). HIV-1 Vpr suppresses the
971 cytomegalovirus promoter in a CRL4(DCAF1) E3 ligase independent manner. *Biochemical and*
972 *Biophysical Research Communications*, 459(2), 214–219.
973 <https://doi.org/10.1016/j.bbrc.2015.02.060>
- 974 Mankan, A. K., Schmidt, T., Chauhan, D., Goldeck, M., Höning, K., Gaidt, M., Kubarenko, A. V.,
975 Andreeva, L., Hopfner, K., & Hornung, V. (2014). Cytosolic RNA:DNA hybrids activate the cGAS
976 –STING axis. *The EMBO Journal*, 33(24), 2937–2946. <https://doi.org/10.15252/embj.201488726>
- 977 Mashiba, M., Collins, D. R., Terry, V. H., & Collins, K. L. (2014). Vpr overcomes macrophage-specific
978 restriction of HIV-1 Env expression and virion production. *Cell Host and Microbe*, 17(3), 414.
979 <https://doi.org/10.1016/j.chom.2014.10.014>
- 980 Matikainen, S., Pirhonen, J., Miettinen, M., Lehtonen, A., Govenius-Vintola, C., Sareneva, T., &
981 Julkunen, I. (2000). Influenza A and sendai viruses induce differential chemokine gene
982 expression and transcription factor activation in human macrophages. *Virology*, 276(1), 138–
983 147. <https://doi.org/10.1006/viro.2000.0542>
- 984 Matsuda, T., & Cepko, C. L. (2004). Electroporation and RNA interference in the rodent retina in vivo
985 and in vitro. *Proceedings of the National Academy of Sciences of the United States of America*,
986 101(1), 16–22. <https://doi.org/10.1073/pnas.2235688100>
- 987 Mesika, A., Grigoreva, I., Zohar, M., & Reich, Z. (2001). A regulated, NF κ B-assisted import of plasmid
988 DNA into mammalian cell nuclei. *Molecular Therapy*, 3(5Pt1), 653–657.
989 <https://doi.org/10.1006/mthe.2001.0312>
- 990 Miller, C. M., Akiyama, H., Agosto, L. M., Emery, A., Ettinger, C. R., Swanstrom, R. I., Henderson, A.
991 J., & Gummuluru, S. (2017). Virion-Associated Vpr Alleviates a Postintegration Block to HIV-1
992 Infection of Dendritic Cells. *Journal of Virology*, 91(13). <https://doi.org/10.1128/JVI.00051-17>
- 993 Miyatake, H., Sanjoh, A., Murakami, T., Murakami, H., Matsuda, G., Hagiwara, K., Yokoyama, M.,
994 Sato, H., Miyamoto, Y., Dohmae, N., & Aida, Y. (2016). Molecular Mechanism of HIV-1 Vpr for
995 Binding to Importin- α . *Journal of Molecular Biology*, 428(13), 2744–2757.
996 <https://doi.org/10.1016/j.jmb.2016.05.003>
- 997 Morellet, N., Bouaziz, S., Petitjean, P., & Roques, B. P. (2003). NMR structure of the HIV-1 regulatory

- 998 protein VPR. *Journal of Molecular Biology*, 285(5), 2105–2117. <https://doi.org/10.1016/S0022->
999 2836(03)00060-3
- 1000 Mori, M., Yoneyama, M., Ito, T., Takahashi, K., Inagaki, F., & Fujita, T. (2004). Identification of Ser-
1001 386 of Interferon Regulatory Factor 3 as Critical Target for Inducible Phosphorylation That
1002 Determines Activation. *Journal of Biological Chemistry*, 279(11), 9698–9702.
1003 <https://doi.org/10.1074/jbc.M310616200>
- 1004 Nitahara-Kasahara, Y., Kamata, M., Yamamoto, T., Zhang, X., Miyamoto, Y., Muneta, K., Iijima, S.,
1005 Yoneda, Y., Tsunetsugu-Yokota, Y., & Aida, Y. (2007). Novel nuclear import of Vpr promoted by
1006 importin α is crucial for human immunodeficiency virus type 1 replication in macrophages.
1007 *Journal of Virology*, 81(10), 5284–5293. <https://doi.org/10.1128/JVI.01928-06>
- 1008 Okumura, A., Alce, T., Lubyova, B., Ezelle, H., Strebler, K., & Pitha, P. M. (2008). HIV-1 accessory
1009 proteins VPR and Vif modulate antiviral response by targeting IRF-3 for degradation. *Virology*,
1010 373(1), 85–97. <https://doi.org/10.1016/j.virol.2007.10.042>
- 1011 Pallett, M. A., Ren, H., Zhang, R.-Y., Scutts, S. R., Gonzalez, L., Zhu, Z., Maluquer de Motes, C., &
1012 Smith, G. L. (2019). Vaccinia Virus BBK E3 Ligase Adaptor A55 Targets Importin-Dependent
1013 NF- κ B Activation and Inhibits CD8 + T-Cell Memory. *Journal of Virology*, 93(10), e00051-19.
1014 <https://doi.org/10.1128/jvi.00051-19>
- 1015 Popov, S., Rexach, M., Zybarth, G., Railing, N., Lee, M.-A., Ratner, L., Lane, C. M., Moore, M. S.,
1016 Blobel, G., & Bukrinsky, M. (1998). Viral protein R regulates nuclear import of the HIV-1 pre-
1017 integration complex. *EMBO Journal*, 17(4), 909–917. <https://doi.org/10.1093/emboj/17.4.909>
- 1018 Rasaiyaah, J., Tan, C. P., Fletcher, A. J., Price, A. J., Blondeau, C., Hilditch, L., Jacques, D. A.,
1019 Selwood, D. L., James, L. C., Noursadeghi, M., & Towers, G. J. (2013). HIV-1 evades innate
1020 immune recognition through specific cofactor recruitment. *Nature*, 503(7476), 402–405.
1021 <https://doi.org/10.1038/nature12769>
- 1022 Rehwinkel, J., Tan, C. P., Goubau, D., Schulz, O., Pichlmair, A., Bier, K., Robb, N., Vreede, F.,
1023 Barclay, W., Fodor, E., & Reis e Sousa, C. (2010). RIG-I Detects Viral Genomic RNA during
1024 Negative-Strand RNA Virus Infection. *Cell*, 140(3), 397–408.
1025 <https://doi.org/10.1016/j.cell.2010.01.020>
- 1026 Schaller, T., Ocwieja, K. E., Rasaiyaah, J., Price, A. J., Brady, T. L., Roth, S. L., Hué, S., Fletcher, A.
1027 J., Lee, K., KewalRamani, V. N., Noursadeghi, M., Jenner, R. G., James, L. C., Bushman, F. D.,
1028 & Towers, G. J. (2011). HIV-1 capsid-cyclophilin interactions determine nuclear import pathway,
1029 integration targeting and replication efficiency. *PLoS Pathogens*, 7(12).
1030 <https://doi.org/10.1371/journal.ppat.1002439>
- 1031 Schirmacher, V. (2015). Signaling through RIG-I and type I interferon receptor: Immune activation by
1032 Newcastle disease virus in man versus immune evasion by Ebola virus (Review). *International*
1033 *Journal of Molecular Medicine*, 36(1), 3–10. <https://doi.org/10.3892/ijmm.2015.2213>
- 1034 Schwefel, D., Groom, H. C. T., Boucherit, V. C., Christodoulou, E., Walker, P. A., Stoye, J. P., Bishop,
1035 K. N., & Taylor, I. A. (2014). Structural basis of lentiviral subversion of a cellular protein
1036 degradation pathway. *Nature*. <https://doi.org/10.1038/nature12815>
- 1037 Servant, M. J., Grandvaux, N., TenOever, B. R., Duguay, D., Lin, R., & Hiscott, J. (2003).

- 1038 Identification of the minimal phosphoacceptor site required for in vivo activation of interferon
1039 regulatory factor 3 in response to virus and double-stranded RNA. *Journal of Biological*
1040 *Chemistry*, 278(11), 9441–9447. <https://doi.org/10.1074/jbc.M209851200>
- 1041 Shaw, G. M., & Hunter, E. (2012). HIV transmission. *Cold Spring Harbor Perspectives in Medicine*,
1042 2(11), a006965. <https://doi.org/10.1101/cshperspect.a006965>
- 1043 Stacey, A. R., Norris, P. J., Qin, L., Haygreen, E. A., Taylor, E., Heitman, J., Lebedeva, M., DeCamp,
1044 A., Li, D., Grove, D., Self, S. G., & Borrow, P. (2009a). Induction of a striking systemic cytokine
1045 cascade prior to peak viremia in acute human immunodeficiency virus type 1 infection, in
1046 contrast to more modest and delayed responses in acute hepatitis B and C virus infections.
1047 *Journal of Virology*, 83(8), 3719–3733. <https://doi.org/10.1128/JVI.01844-08>
- 1048 Stacey, A. R., Norris, P. J., Qin, L., Haygreen, E. A., Taylor, E., Heitman, J., Lebedeva, M., DeCamp,
1049 A., Li, D., Grove, D., Self, S. G., & Borrow, P. (2009b). Induction of a Striking Systemic Cytokine
1050 Cascade prior to Peak Viremia in Acute Human Immunodeficiency Virus Type 1 Infection, in
1051 Contrast to More Modest and Delayed Responses in Acute Hepatitis B and C Virus Infections.
1052 *Journal of Virology*, 83(8), 3719–3733. <https://doi.org/10.1128/jvi.01844-08>
- 1053 Su, J., Rui, Y., Lou, M., Yin, L., Xiong, H., Zhou, Z., Shen, S., Chen, T., Zhang, Z., Zhao, N., Zhang,
1054 W., Cai, Y., Markham, R., Zheng, S., Xu, R., Wei, W., & Yu, X.-F. (2019). HIV-2/SIV Vpx targets
1055 a novel functional domain of STING to selectively inhibit cGAS–STING-mediated NF-κB
1056 signalling. *Nature Microbiology*, 4(12), 2552–2564. <https://doi.org/10.1038/s41564-019-0585-4>
- 1057 Suhara, W., Yoneyama, M., Iwamura, T., Yoshimura, S., Tamura, K., Namiki, H., Aimoto, S., & Fujita,
1058 T. (2000). Analyses of virus-induced homomeric and heteromeric protein associations between
1059 IRF-3 and coactivator CBP/p300. *Journal of Biochemistry*, 128(2), 301–307.
1060 <https://doi.org/10.1093/oxfordjournals.jbchem.a022753>
- 1061 Sumner, R.P., Thorne, L. G., Fink, D. L., Khan, H., Milne, R. S., & Towers, G. J. (2017). Are evolution
1062 and the intracellular innate immune system key determinants in HIV transmission? *Frontiers in*
1063 *Immunology*, 8(OCT). <https://doi.org/10.3389/fimmu.2017.01246>
- 1064 Sumner, Rebecca P, Harrison, L., Touizer, E., Peacock, T. P., Spencer, M., Zuliani-Alvarez, L., &
1065 Towers, G. J. (2019). Disrupting HIV-1 capsid formation causes cGAS sensing of viral DNA.
1066 *BioRxiv*, 838011. <https://doi.org/10.1101/838011>
- 1067 Taylor, S. L., Frias-Staheli, N., Garcia-Sastre, A., & Schmaljohn, C. S. (2009). Hantaan Virus
1068 Nucleocapsid Protein Binds to Importin Proteins and Inhibits Tumor Necrosis Factor Alpha-
1069 Induced Activation of Nuclear Factor Kappa B. *Journal of Virology*, 83(3), 1271–1279.
1070 <https://doi.org/10.1128/jvi.00986-08>
- 1071 Trotard, M., Tsopoulidis, N., Tibroni, N., Willemsen, J., Binder, M., Ruggieri, A., & Fackler, O. T.
1072 (2016). Sensing of HIV-1 Infection in Tzm-bl Cells with Reconstituted Expression of STING.
1073 *Journal of Virology*. <https://doi.org/10.1128/jvi.02966-15>
- 1074 Vermeire, J., Roesch, F., Sauter, D., Rua, R., Hotter, D., Van Nuffel, A., Vanderstraeten, H.,
1075 Naessens, E., Iannucci, V., Landi, A., Witkowski, W., Baeyens, A., Kirchhoff, F., & Verhasselt, B.
1076 (2016). HIV Triggers a cGAS-Dependent, Vpu- and Vpr-Regulated Type I Interferon Response
1077 in CD4+ T Cells. *Cell Reports*, 17(2), 413–424. <https://doi.org/10.1016/j.celrep.2016.09.023>

- 1078 Vermeire, Jolien, Naessens, E., Vanderstraeten, H., Landi, A., Iannucci, V., van Nuffel, A., Taghon,
1079 T., Pizzato, M., & Verhasselt, B. (2012). Quantification of Reverse Transcriptase Activity by
1080 Real-Time PCR as a Fast and Accurate Method for Titration of HIV, Lenti- and Retroviral
1081 Vectors. *PLoS ONE*, 7(12), e50859. <https://doi.org/10.1371/journal.pone.0050859>
- 1082 Vodicka, M. A., Koepp, D. M., Silver, P. A., & Emerman, M. (1998). HIV-1 Vpr interacts with the
1083 nuclear transport pathway to promote macrophage infection. *Genes and Development*, 12(2),
1084 175–185. <https://doi.org/10.1101/gad.12.2.175>
- 1085 Wu, Y., Zhou, X., Barnes, C. O., DeLucia, M., Cohen, A. E., Gronenborn, A. M., Ahn, J., & Calero, G.
1086 (2016). The DDB1-DCAF1-Vpr-UNG2 crystal structure reveals how HIV-1 Vpr steers human
1087 UNG2 toward destruction. *Nature Structural and Molecular Biology*, 23(10), 933–939.
1088 <https://doi.org/10.1038/nsmb.3284>
- 1089 Xia, T., Konno, H., Ahn, J., & Barber, G. N. (2016). Deregulation of STING Signaling in Colorectal
1090 Carcinoma Constrains DNA Damage Responses and Correlates With Tumorigenesis. *Cell*
1091 *Reports*, 14(2), 282–297. <https://doi.org/10.1016/j.celrep.2015.12.029>
- 1092 Xia, T., Konno, H., & Barber, G. N. (2016). Recurrent Loss of STING Signaling in Melanoma
1093 Correlates with Susceptibility to Viral Oncolysis. *Cancer Research*, 76(22), 6747–6759.
1094 <https://doi.org/10.1158/0008-5472.CAN-16-1404>
- 1095 Xu, S., Ducroux, A., Ponnurangam, A., Vieyres, G., Franz, S., Müsken, M., Zillinger, T., Malassa, A.,
1096 Ewald, E., Hornung, V., Barchet, W., Häussler, S., Pietschmann, T., & Goffinet, C. (2016).
1097 cGAS-Mediated Innate Immunity Spreads Intercellularly through HIV-1 Env-Induced Membrane
1098 Fusion Sites. *Cell Host and Microbe*, 20(4), 443–457.
1099 <https://doi.org/10.1016/j.chom.2016.09.003>
- 1100 Xu, W., Edwards, M. R., Borek, D. M., Feagins, A. R., Mittal, A., Alinger, J. B., Berry, K. N., Yen, B.,
1101 Hamilton, J., Brett, T. J., Pappu, R. V., Leung, D. W., Basler, C. F., & Amarasinghe, G. K.
1102 (2014). Ebola virus VP24 targets a unique NLS binding site on karyopherin alpha 5 to selectively
1103 compete with nuclear import of phosphorylated STAT1. *Cell Host and Microbe*, 16(2), 187–200.
1104 <https://doi.org/10.1016/j.chom.2014.07.008>
- 1105 Yamashita, M., & Emerman, M. (2005). The cell cycle independence of HIV infections is not
1106 determined by known karyophilic viral elements. *PLoS Pathogens*, 1(3), e18–e18.
1107 <https://doi.org/10.1371/journal.ppat.0010018>
- 1108 Yan, J., Shun, M. C., Zhang, Y., Hao, C., & Skowronski, J. (2019). HIV-1 Vpr counteracts HLTF-
1109 mediated restriction of HIV-1 infection in T cells. *Proceedings of the National Academy of*
1110 *Sciences of the United States of America*, 116(7), 9568–9577.
1111 <https://doi.org/10.1073/pnas.1818401116>
- 1112 Yan, N., Regalado-Magdos, A. D., Stiggelbout, B., Lee-Kirsch, M. A., & Lieberman, J. (2010). The
1113 cytosolic exonuclease TREX1 inhibits the innate immune response to human immunodeficiency
1114 virus type 1. *Nature Immunology*, 11(11), 1005–1013. <https://doi.org/10.1038/ni.1941>
- 1115 Ye, J., Chen, Z., Li, Y., Zhao, Z., He, W., Zohaib, A., Song, Y., Deng, C., Zhang, B., Chen, H., & Cao,
1116 S. (2017). Japanese Encephalitis Virus NS5 Inhibits Type I Interferon (IFN) Production by
1117 Blocking the Nuclear Translocation of IFN Regulatory Factor 3 and NF-κB. *Journal of Virology*,

- 1118 91(8), e00039-17. <https://doi.org/10.1128/jvi.00039-17>
- 1119 Yoneyama, M., Suhara, W., Fukuhara, Y., Fukuda, M., Nishida, E., & Fujita, T. (1998). Direct
1120 triggering of the type I interferon system by virus infection: Activation of a transcription factor
1121 complex containing IRF-3 and CBP/p300. *EMBO Journal*, 17(4), 1087–1095.
1122 <https://doi.org/10.1093/emboj/17.4.1087>
- 1123 Zander, K., Sherman, M. P., Tessmer, U., Bruns, K., Wray, V., Prechtel, A. T., Schubert, E., Henklein,
1124 P., Luban, J., Neidleman, J., Greene, W. C., & Schubert, U. (2003). Cyclophilin A Interacts with
1125 HIV-1 Vpr and Is Required for Its Functional Expression. *Journal of Biological Chemistry*,
1126 278(44), 43202–43213. <https://doi.org/10.1074/jbc.M305414200>
- 1127 Zhang, C., Shang, G., Gui, X., Zhang, X., Bai, X. chen, & Chen, Z. J. (2019). Structural basis of
1128 STING binding with and phosphorylation by TBK1. In *Nature* (pp. 567(7748):394-398).
1129 <https://doi.org/10.1038/s41586-019-1000-2>
- 1130 Zhang, F., & Bieniasz, P. D. (2019). HIV-1 Vpr induces cell cycle arrest and enhances viral gene
1131 expression by depleting CCDC137. *BioRxiv*, 2019.12.24.888230.
1132 <https://doi.org/10.1101/2019.12.24.888230>
- 1133 Zhang, S., Feng, Y., Narayan, O., & Zhao, L. J. (2001). Cytoplasmic retention of HIV-1 regulatory
1134 protein V pr by protein-protein interaction with a novel human cytoplasmic protein VprBP. *Gene*,
1135 263(1–2), 131–140. [https://doi.org/10.1016/S0378-1119\(00\)00583-7](https://doi.org/10.1016/S0378-1119(00)00583-7)
- 1136 Zhu, H., Jian, H., & Zhao, L. J. (2004). Identification of the 15FRFG domain in HIV-1 Gag p6 essential
1137 for Vpr packaging into the virion. *Retrovirology*, 1(26), 343–398. <https://doi.org/10.1186/1742-4690-1-26>
- 1139 Zila, V., Müller, T. G., Laketa, V., Müller, B., & Kräusslich, H. G. (2019). Analysis of CA content and
1140 CPSF6 dependence of early HIV-1 replication complexes in SupT1-R5 cells. *MBio*, 10(6),
1141 e02501-19. <https://doi.org/10.1128/mBio.02501-19>
- 1142 Zufferey, R., Nagy, D., Mandel, R. J., Naldini, L., & Trono, D. (1997). Multiply attenuated lentiviral
1143 vector achieves efficient gene delivery in vivo. *Nature Biotechnology*, 15(9), 871–875.
1144 <https://doi.org/10.1038/nbt0997-871>
- 1145

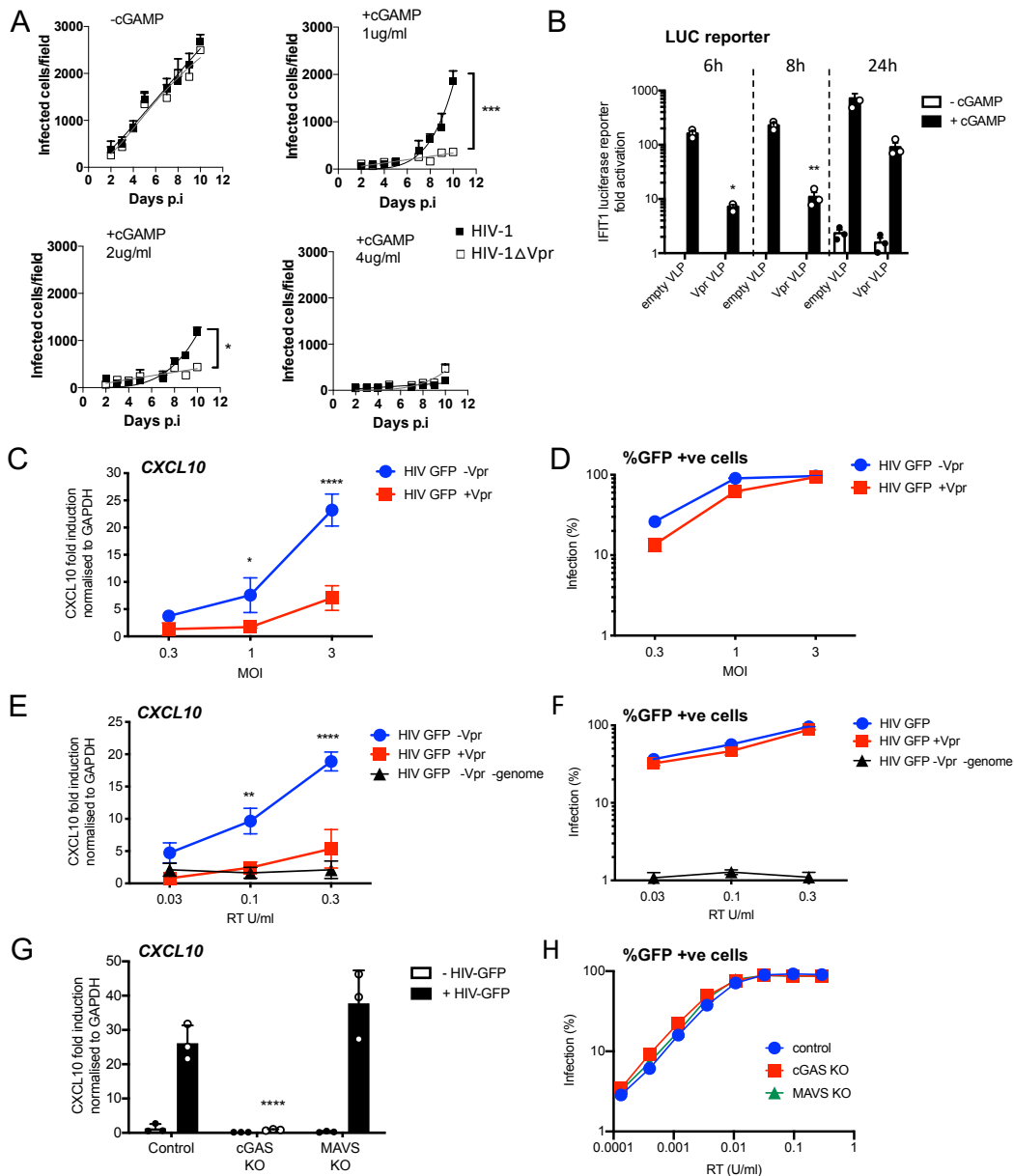


Figure 1 HIV-1 replication in cGAMP stimulated MDMs requires Vpr

(A) Replication of WT Yu2 HIV-1 or Yu2 HIV-1ΔVpr in MDMs stimulated with 1 µg/ml, 2 µg/ml or 4 µg/ml cGAMP or left unstimulated, infection measured by counting Gag positive cells stained with anti-p24. Mean±SEM n=3 1 and 2 µg/ml cGAMP; n=2 4 µg/ml cGAMP. *** = 2 way ANOVA p value <0.001, * = p<0.05. (B) Fold induction of IFIT1-Luc after activation of STING by cGAMP (5 µg/ml) and infection with HIV-1 virus like particles (VLP) lacking genome and bearing Vpr (+Vpr) or lacking Vpr (-Vpr) (1 RT U/ml) in IFIT1-Luc reporter THP-1 cells. cGAMP and virus were added to cells at the same time. (C) Fold induction of *CXCL10* after infection of THP-1 cells with HIV-GFP -Vpr or HIV-GFP +Vpr at the indicated MOI. (D) Percentage of THP-1 cells infected by HIV-GFP -Vpr or HIV-GFP +Vpr in (C). (E) Fold induction of *CXCL10* after infection of THP-1 cells with HIV-GFP -Vpr, HIV-GFP +Vpr or HIV-1 particles lacking Vpr and genome, at indicated doses measured by reverse transcriptase SG-PERT assay. (F) Percentage of THP-1 cells infected by HIV-GFP viruses in (E). (G) Fold induction of *CXCL10* after infection of unmodified control, cGAS^{-/-} or MAVS^{-/-} THP-1 knock out cells with HIV-GFP lacking Vpr (0.3 RT U/ml). (H) Percentage infection of control, cGAS^{-/-} or MAVS^{-/-} THP-1 knockout cells infected with HIV-GFP at indicated doses of RT (SG-PERT).

(B-H) Data are expressed as means ± SD (n = 3) with two-way ANOVA * (p<0.05), ** (p<0.01), *** (p<0.001), **** (p<0.0001) compared to virus without genome (B), HIV GFP+Vpr (C, E) and control (G).

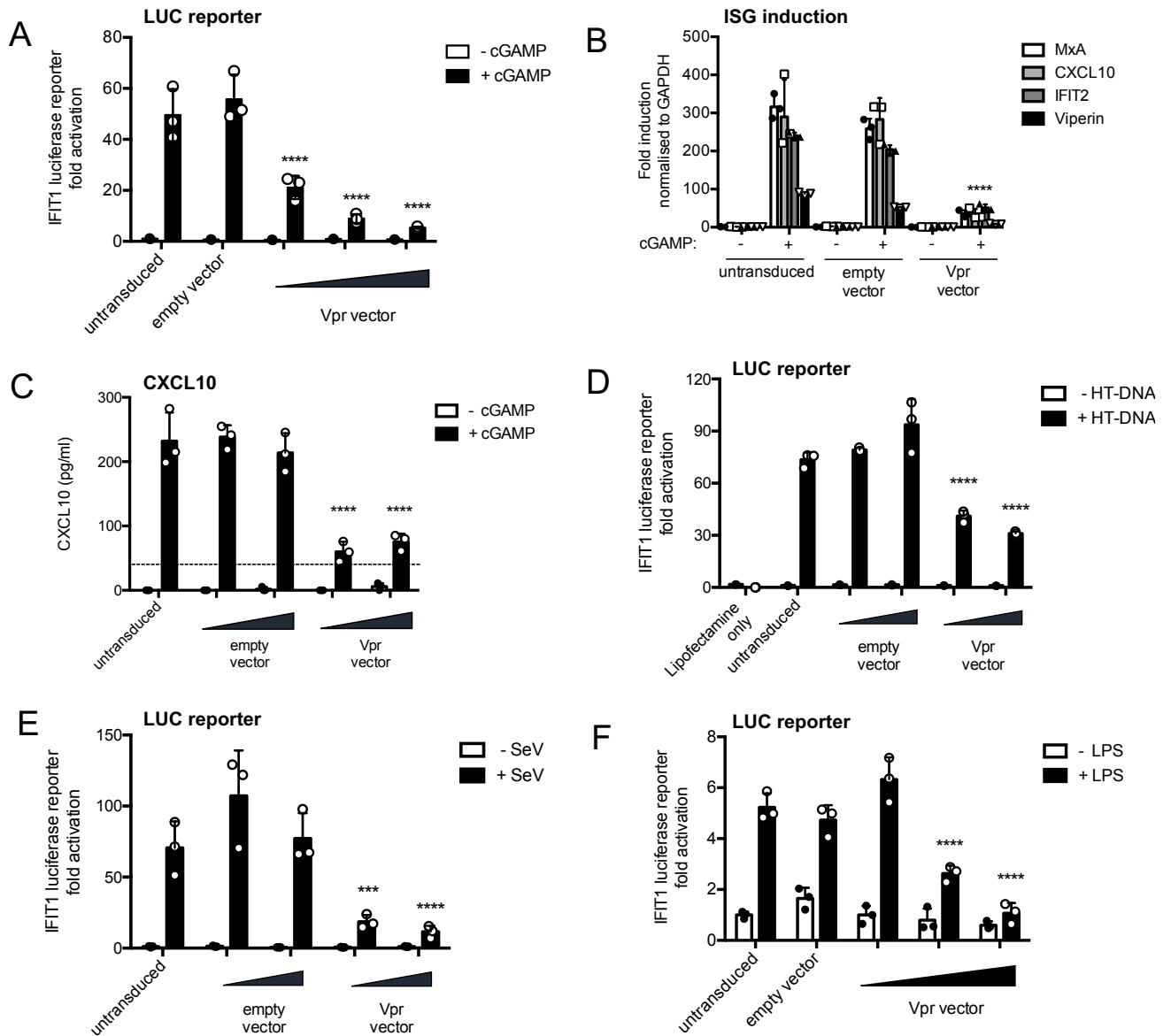


Figure 2 HIV-1 Vpr expression inhibits interferon stimulated gene expression after stimulation with various innate immune stimuli

(A) Fold induction of IFIT1-Luc, after activation of STING by cGAMP (5 μ g/ml), in IFIT1-Luc reporter THP-1 cells expressing Vpr from a lentiviral vector delivered at MOIs of 0.25, 0.5, 1, or after empty vector transduction (MOI 1) or in untransduced cells. (B) Fold induction of ISGs *MxA*, *CXCL10*, *IFIT2* and *Viperin* after activation of STING by cGAMP (5 μ g/ml) in cells expressing Vpr from a lentiviral vector (MOI 1), or after empty vector transduction (MOI 1) or in untransduced THP-1 cells. (C) Secreted CXCL10 (ELISA) after activation of STING by cGAMP (5 μ g/ml) in cells expressing Vpr from a lentiviral vector (MOI 0.5, 1), or after transduction with empty vector (MOI 0.5, 1) or in untransduced THP-1 cells. Dotted line shows limit of detection. (D) Fold induction of IFIT1-Luc after HT-DNA transfection (5 μ g/ml) of cells expressing Vpr from a lentiviral vector (MOI 0.5, 1), or empty vector (MOI 0.5, 1) or in untransduced IFIT1-Luc reporter THP-1 cells. (E) Fold induction of IFIT1-Luc, after Sendai virus infection, of cells expressing Vpr from a lentiviral vector (MOI 0.5, 1), or after transduction by empty vector (MOI 0.5, 1) or in untransduced IFIT1-Luc reporter THP-1 cells. (F) Fold induction of IFIT1-Luc, after LPS treatment (1 μ g/ml), of cells expressing Vpr from a lentiviral vector (MOI 0.25, 0.5, 1), after transduction by empty vector (MOI 1) or in untransduced IFIT1-Luc reporter THP-1 cells. Data are expressed as mean \pm SD (n = 3) analysed using two-way ANOVA * (p<0.05), ** (p<0.01), *** (p<0.001), **** (p<0.0001) compared to data for empty vector. n= 3 (A, D-F) or 2 (B-C) independent experiments.

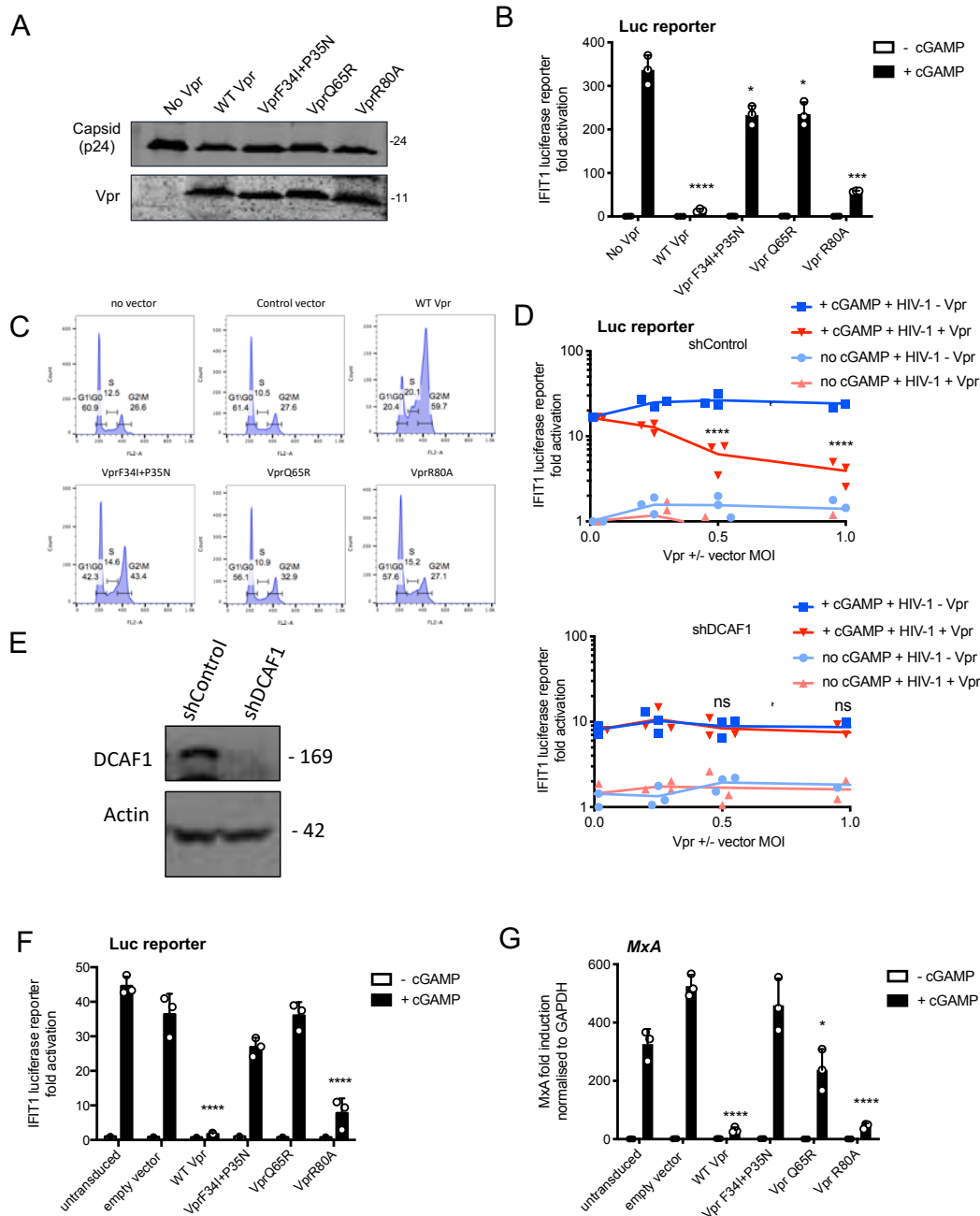


Figure 3 Vpr inhibition of innate immune activation is dependent on DCAF1 but independent of cell cycle arrest

(A) Immunoblot detecting p24 (capsid) or Vpr in pelleted VSV-G pseudotyped VLP lacking genome used in (B). (B) Fold induction of IFIT1-Luc after activation of STING by cGAMP (5 μ g/ml) and infection with VLP bearing WT or mutant Vpr, or lacking Vpr (1 RT U/ml) in THP-1. Cells were infected at the same time as cGAMP treatment. (C) Flow cytometry showing cell cycle phases of THP-1 transduced with an empty vector, WT Vpr, or mutant Vpr, encoding vector (MOI 1) or left untransduced as a control, stained with propidium iodide to label DNA. Percentage cells in each cell cycle stage are shown. (D) Fold induction of IFIT1-Luc after activation of STING by cGAMP (5 μ g/ml) in cells expressing Vpr from a lentiviral vector, or expressing empty vector, or in untransduced THP-1 expressing a control, or a DCAF1 targeting shRNA. Mean \pm -SEM n=3 independent experiments. (E) Immunoblot detecting DCAF1, or actin as a loading control, from extracted THP-1 cells expressing a non-targeting, or DCAF1-targeting, shRNA. (F) Fold induction of IFIT1-Luc after activation of STING by cGAMP (5 μ g/ml) in cells expressing WT, or mutant, Vpr from a lentiviral vector (MOI 1), or empty vector (MOI 1) or in untransduced THP-1. (G) Fold induction of *MxA* mRNA after activation of STING by cGAMP (5 μ g/ml) in cells

expressing WT, or mutant, Vpr from a lentiviral vector (MOI 1), or after transduction by empty vector (MOI 1) or in untransduced THP-1. Data are mean \pm SD (n = 3). Two-way ANOVA: * (p<0.05), ** (p<0.01), *** (p<0.001), **** (p<0.0001) compared to no Vpr or empty vector controls. Data are representative of three (B-D, F) or two (A, E, G) independent experiments.

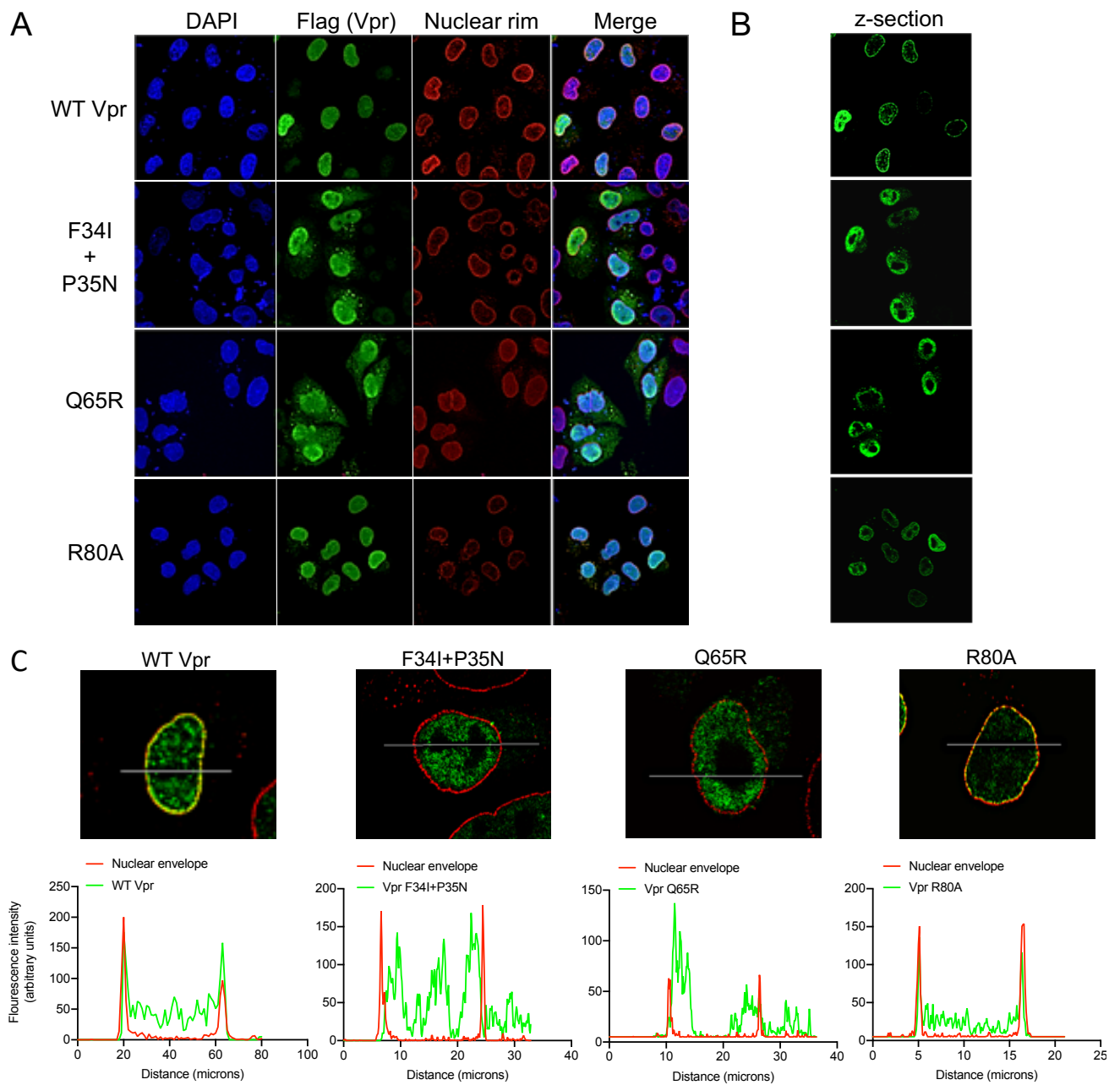


Figure 4 Wild Type Vpr, but not sensing antagonism inactive Vpr mutants, localise to nuclear pores

(A) Immunofluorescence confocal projections of HeLa cells transfected with Flag-tagged WT, or mutant, Vpr encoded by pcDNA3.1 plasmid (50 ng) and stained using antibodies detecting the Flag-tag (green) or nuclear pore complex (mab414) (red). 4',6-Diamidino-2-phenylindole dihydrochloride (DAPI) stains nuclear DNA (Blue). (B) Selected confocal images (z-section) of cells in (A) showing effect of Vpr mutation on Vpr colocalization with mab414 nuclear pore staining. (C) Assessment of colocalization of Vpr with mab414 nuclear pore staining.

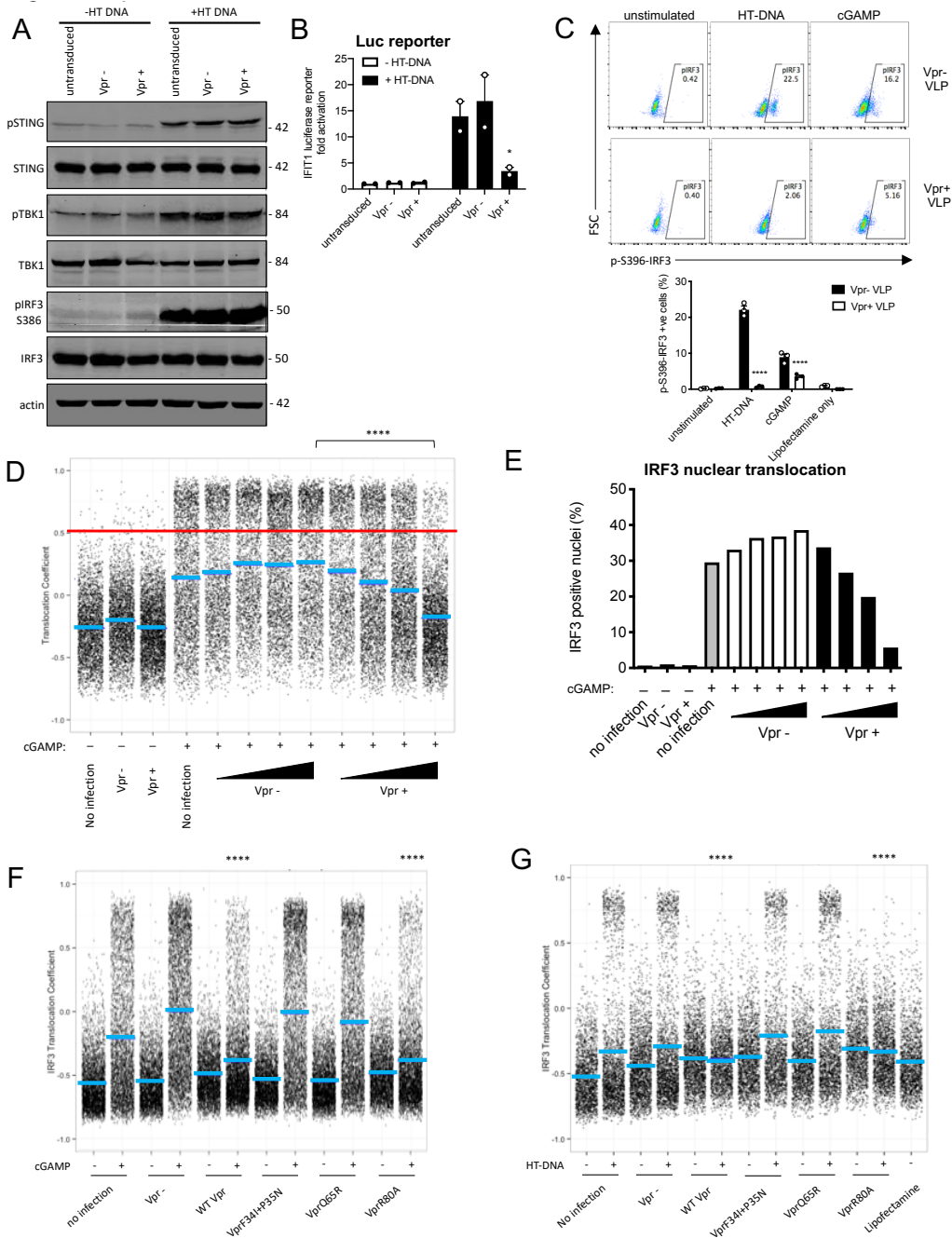


Figure 5 Vpr inhibits IRF3 nuclear translocation

(A) Immunoblot detecting Phospho-STING (Ser366), total STING, phospho-TBK1 (Ser172), total TBK1, phospho-IRF3 (Ser386), total IRF3, or actin as a loading control, from extracted THP-1 cells expressing Vpr from a lentiviral vector, or empty vector (MOI 1), or THP-1 left untransduced as a control and transfected with HT-DNA (5 μ g/ml) or left untransfected as a control. Size markers are shown in kDa. (B) Mean fold induction of IFIT1-Luc in cells from Figure 5A and Figure S5B (C) Flow cytometry plot (forward scatter vs pIRF3-S396 fluorescence) of THP-1 cells stimulated with cGAMP (5 μ g/ml) or HT-DNA transfection (5 μ g/ml) and then immediately infected with Vpr bearing virus-like particles (VLP) lacking genome (1 RT U/ml), or Vpr free VLP and fixed three hours after infection. Lower panel shows the flow cytometry data as a bar graph, plotting pIRF3-S396 positive cells. (D) Single cell immunofluorescence measurement of IRF3 nuclear translocation in PMA differentiated THP-1 cells treated with cGAMP, or left untreated, and then immediately infected with HIV-1 GFP bearing Vpr, lacking Vpr or left untransduced. Cells were fixed and stained three hours after infection. Red line shows the translocation coefficient threshold. Blue lines represent mean translocation coefficient. (E) Percentage of cells in Figure 5D with IRF3 translocation coefficient greater than 0.5 (above red line). (F) Single cell

immunofluorescence measurement of IRF3 nuclear translocation in PMA differentiated THP-1 cells stimulated with cGAMP (5 µg/ml), or left unstimulated, and then immediately infected with HIV-1 GFP lacking Vpr or bearing WT Vpr or Vpr mutants as shown (1 RT U/ml) or left uninfected. (G) Single cell immunofluorescence measurement of IRF3 nuclear translocation in PMA differentiated THP-1 cells transfected with HT-DNA (5 µg/ml), or left untransfected, and immediately infected with HIV-1 GFP lacking Vpr, or bearing WT or mutant Vpr (1 RT U/ml) or left uninfected.

Data in B is expressed as means ± SEM (n = 2). Data is analysed using two-way ANOVA: * (p<0.05), ** (p<0.01), *** (p<0.001), **** (p<0.0001) compared to data from infection with HIV-1 lacking Vpr. Data are representative of three (C–G) or two (A, B) independent experiments.

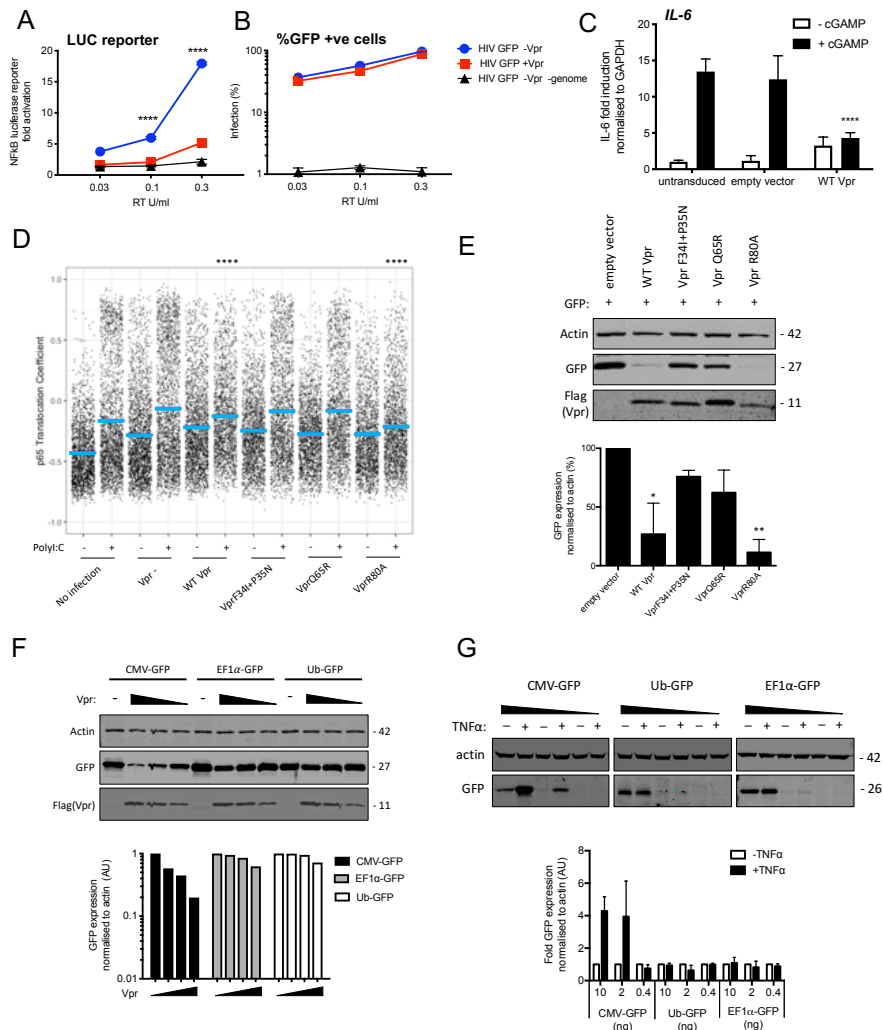


Figure 6 Vpr inhibits NF- κ B p65 nuclear translocation and NF- κ B sensitive plasmid expression

(A) Fold induction of NF- κ B-Luc after infection of THP-1 cells with HIV-GFP lacking Vpr, HIV-GFP bearing Vpr, or HIV-GFP lacking Vpr and genome, at the indicated doses. (B) Percentage of THP-1 cells in (A). (C) Fold induction of *IL-6* after activation of STING by cGAMP (5 μ g/ml) in cells expressing empty vector or Vpr encoding vector (MOI 1), or in untransduced THP-1 cells. (D) Single cell immunofluorescence measurement of NF- κ B (p65) nuclear translocation in PMA differentiated THP-1 cells transfected with Poly I:C (50 ng/ml), or left untreated, and infected with HIV-1 GFP lacking Vpr, HIV-1 GFP bearing Vpr (1 RT U/ml) or left uninfected. Cells were stained three hours after transfection and infection. (E) Immunoblot detecting Flag-Vpr, GFP, or actin as a loading control, from HEK293T cells transfected with 50 ng of empty vector, Flag-tagged WT Vpr vector, or Flag-tagged mutant Vpr vector, and CMV-GFP vector (50 ng). Size markers are shown in kDa. GFP expression from two independent immunoblots was quantified by densitometry and is shown in the lower panel. (F) Immunoblot detecting Flag-Vpr, GFP, or actin as a loading control, from HEK293T cells transfected with empty vector (200 ng) or Vpr vector (50ng, 100ng, 200ng) and CMV-GFP, EF1 α -GFP or Ub-GFP plasmids (50 ng). Size markers are shown in kDa. GFP expression quantified by densitometry is shown in the lower panel. (G) Immunoblot detecting GFP, or actin as a loading control, from HEK293T cells transfected with CMV-GFP, EF1 α -GFP or Ub-GFP plasmids (10 ng, 2 ng, 0.4 ng) and stimulated with TNF α (200 ng/ml) or left unstimulated. Size markers are shown in kDa. GFP expression, from two independent immunoblots, quantified by densitometry, is shown in the lower panel. Data in (A, B, C) is expressed as mean \pm SD (n = 3). Data in (E, F, G) is expressed as mean \pm SD (n=2). Two-way ANOVA: * (p<0.05), ** (p<0.01), *** (p<0.001), **** (p<0.0001) compared to empty vector or HIV GFP+Vpr.

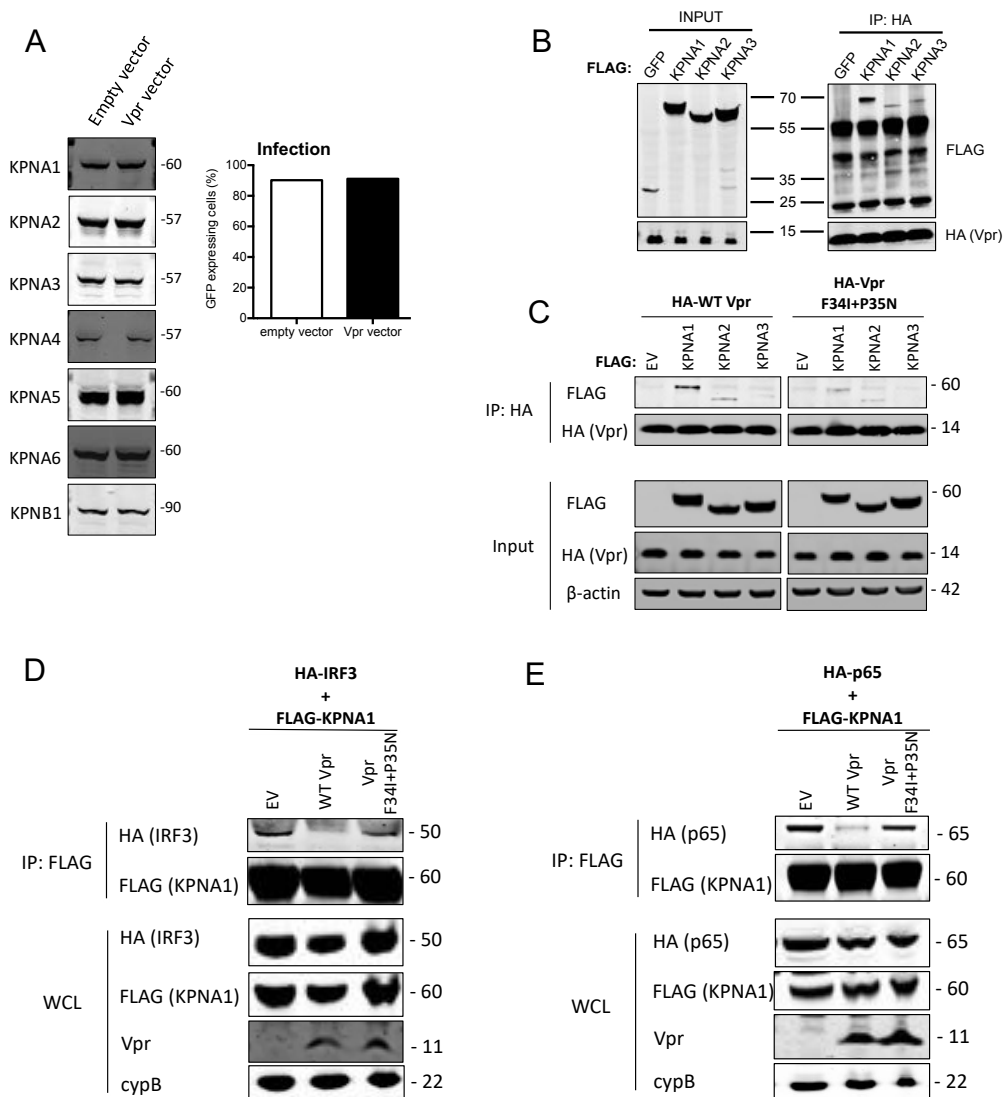


Figure 7 HIV-1 Vpr interacts with karyopherins and inhibits IRF3/NF- κ B(p65) recruitment to KPNA1

(A) Immunoblot detecting KPNA1-6 or KPNB1 from extracted HEK293T cells infected with empty vector, or Vpr encoding vector at a dose of 0.05 RT U/ml (MOI=2). Size markers are shown in kDa. Percentage infection by HIV-1 GFP bearing Vpr encoding or empty vector is shown on the right. (B) Co-immunoprecipitation of Flag-KPNA1-3 and HA-Vpr. Input shows immunoblot detecting extracted HEK293T whole cell lysates expressing flag-KPNA1-3, flag-GFP and HA-Vpr before immunoprecipitation. Co-immunoprecipitation precipitates Vpr with HA-beads and detects Flag-KPNA1-3. (C) Co-immunoprecipitation of Flag-KPNA1-3 and WT HA-Vpr or HA-Vpr F34I+P35N. Input shows immunoblots detecting HA-Vpr or Flag-KPNA1-3 in extracted HEK293T whole cell lysates (WCL) before immunoprecipitation. β -Actin is detected as a loading control. Co-immunoprecipitation precipitates Vpr with HA-beads and detects Flag-KPNA1-3. (D) Co-immunoprecipitation of HA-IRF3 and Flag-KPNA1 in the presence and absence of WT Vpr or Vpr F34I+P35N to detect competition between Vpr and IRF3 for KPNA1. Input shows immunoblots detecting HA-IRF3 or Flag-KPNA1 or Vpr in extracted HEK293T whole cell lysates (WCL) before immunoprecipitation. CypB is detected as a loading control. Co-immunoprecipitation precipitates KPNA1 with Flag-beads and detects HA-IRF3 in the presence and absence of WT Vpr or inactive Vpr F34I+P35N. (E) Co-immunoprecipitation of HA-p65 and Flag-KPNA1 in the presence and absence of WT Vpr or Vpr F34I+P35N to detect competition between Vpr and p65 for KPNA1. Input shows immunoblots detecting HA-p65 or Flag-KPNA1 or Vpr in extracted HEK293T whole cell lysates (WCL) before immunoprecipitation. CypB is detected as a loading control. Co-immunoprecipitation precipitates KPNA1 with Flag-beads and detects HA-p65 in the presence and absence of WT Vpr or Vpr F34I+P35N.